

Electronic Supplementary Information

**Tricarbocyanine-*N*-triazoles: The Scaffold-of-Choice for Long-Term Near-Infrared Imaging
of Immune Cells *in vivo***

Richard J. Mellanby, Jamie I. Scott, Iris Mair, Antonio Fernandez, Louise Saul, Jochen Arlt, Monica Moral, Marc Vendrell

Table of Contents:

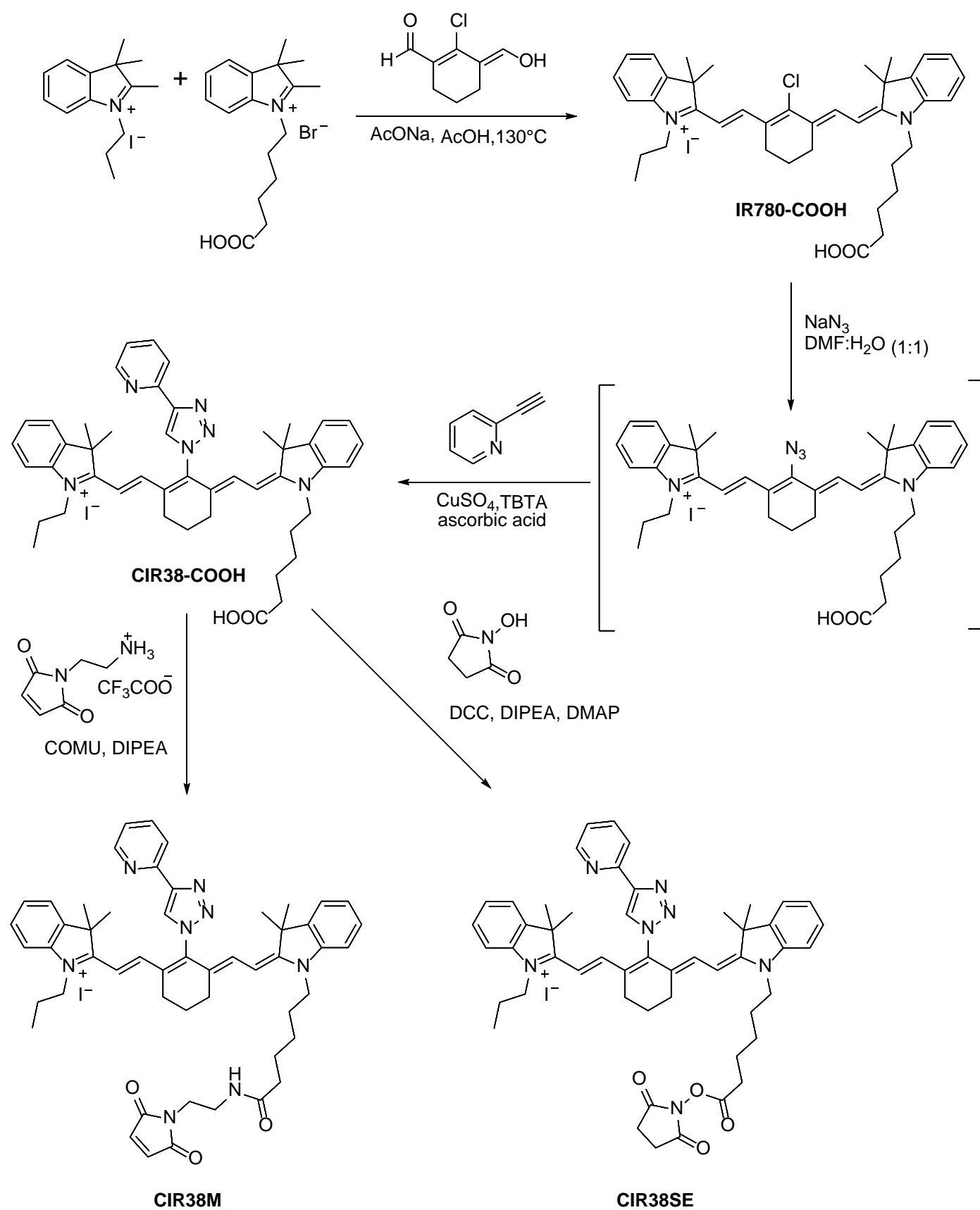
Supplementary Methods and NMR spectra

Supplementary Schemes

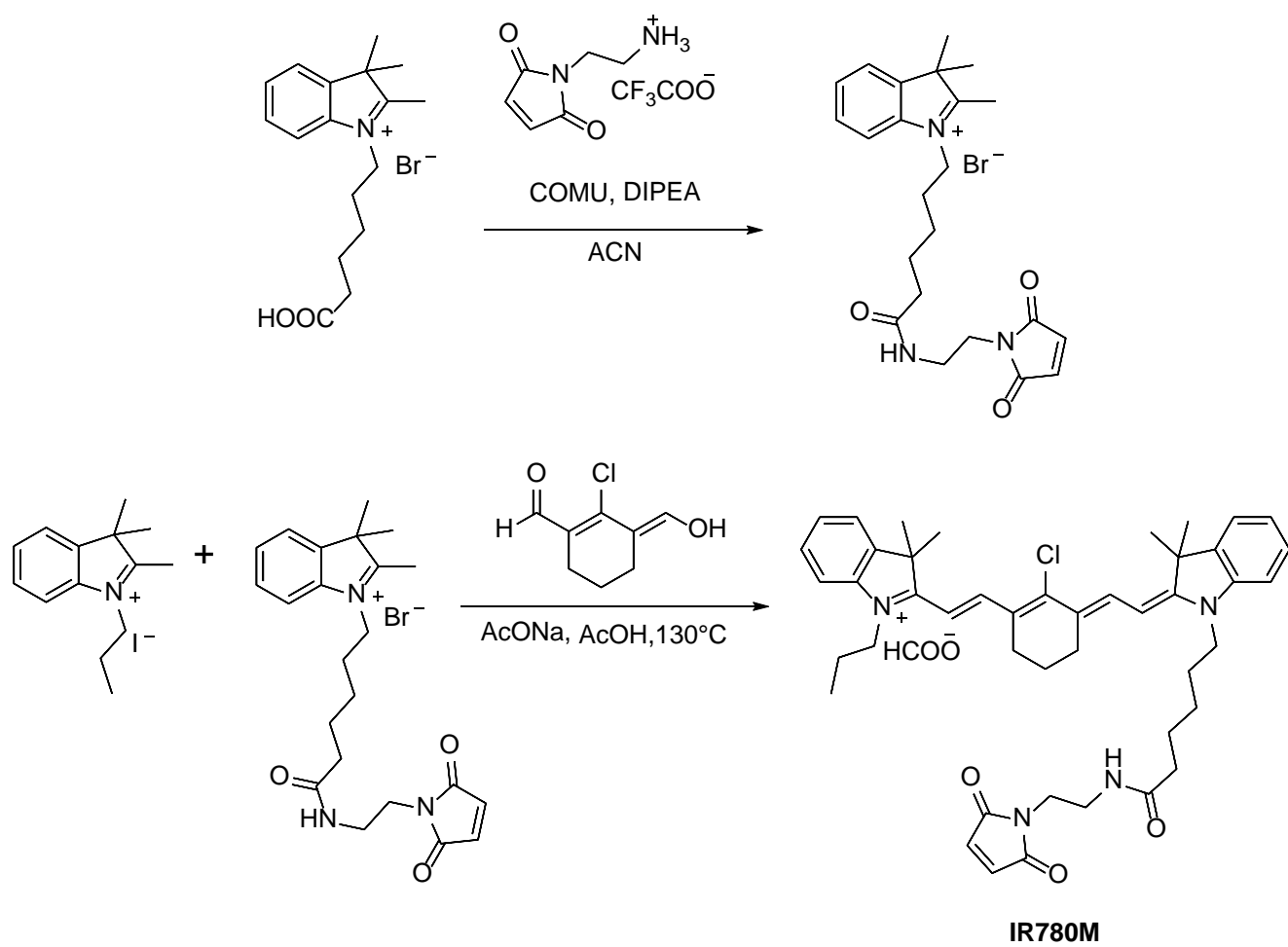
Supplementary Figures

Supplementary Tables

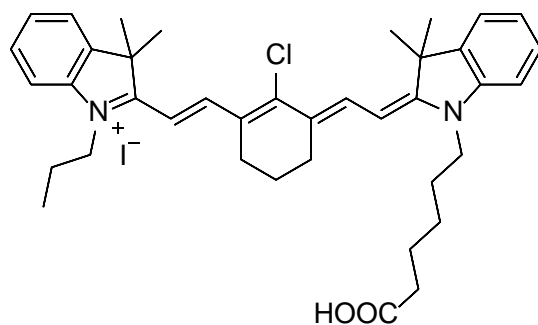
Supplementary Methods



Scheme S1. Synthetic scheme for the preparation of **CIR38** derivatives.



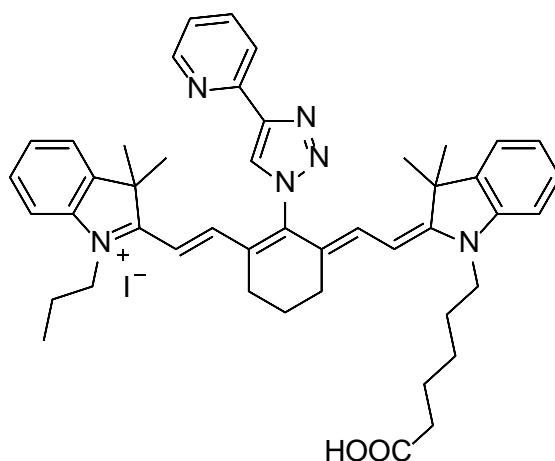
Scheme S2. Synthetic scheme for the preparation of IR780-maleimide (**IR780M**).



IR780-COOH

IR780-COOH. To a solution of sodium acetate (258 mg, 3.15 mmol) in AcOH (20 mL) was added 2-chloro-3-(hydroxymethylene)-1-cyclohexene-1-carboxaldehyde (86 mg, 0.5 mmol) and 3*H*-indolium,1-(5-carboxypentyl)-2,3,3-trimethylbromide (214 mg, 0.6 mmol). The resulting solution was stirred at 130 °C under reflux for 2 h. To the reaction was then added 3*H*-indolium,2,3,3-trimethyl-1-propyl iodide (148 mg, 0.5 mmol) and the mixture was stirred overnight at 130 °C. The reaction was then cooled to r.t. and solvents were evaporated under reduced pressure. The resulting crude was then purified by column chromatography (CH₂Cl₂: MeOH, 98:2) to isolate **IR780-COOH** as a green solid (120 mg, 32% yield).

¹H NMR (500 MHz, MeOD) δ 8.45 (dd, *J* = 14.1, 5.0 Hz, 2H), 7.57 – 7.51 (m, 2H), 7.44 (ddt, *J* = 8.4, 7.5, 1.1 Hz, 2H), 7.38 – 7.33 (m, 2H), 7.30 (tdt, *J* = 7.4, 3.0, 0.9 Hz, 2H), 6.31 (dd, *J* = 14.1, 9.5 Hz, 2H), 4.19 (dt, *J* = 9.9, 7.5 Hz, 4H), 2.75 (t, *J* = 6.3 Hz, 3H), 2.32 (t, *J* = 7.3 Hz, 2H), 1.99 (s, 3H), 1.94 – 1.86 (m, 4H), 1.80 (d, *J* = 2.8 Hz, 1H), 1.74 (s, 10H), 1.73 – 1.67 (m, 2H), 1.63 (s, 1H), 1.56 – 1.48 (m, 2H), 1.07 (t, *J* = 7.4 Hz, 3H). **¹³C NMR** (126 MHz, MeOD) δ 176.3, 174.2, 173.1, 172.8, 149.7, 144.2, 144.0, 142.3, 142.2, 141.2, 141.2, 132.8, 132.8, 129.8, 129.1, 128.5, 128.5, 126.6, 125.2, 125.1, 123.3, 122.1, 115.2, 111.0, 110.9, 101.1, 100.9, 53.4, 45.4, 43.7, 33.6, 27.0, 26.0, 24.4, 21.5, 20.7, 20.5, 19.6, 10.3.



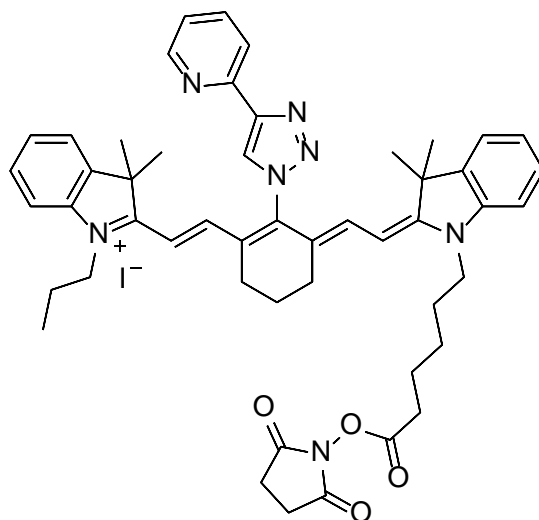
CIR38-COOH

CIR38-COOH. To a solution of **IR780-COOH** (57 mg, 0.08 mmol) in DMF (1 mL) was added sodium azide (25 mg, 0.4 mmol) in H₂O (1 mL). The resulting mixture was stirred at r. t. for 20 min. To the reaction was then added 2-ethynylpyridine (79 mg, 0.8 mmol), CuSO₄ (25 mg, 0.16 mmol), TBTA (85 mg, 0.16 mmol) and sodium ascorbate (32 mg, 0.16 mmol) and the mixture was stirred at r. t. for 2 h. The reaction crude was diluted in CH₂Cl₂ (20 mL), and the organic phase was washed with H₂O (3 × 10 mL). The organic extracts were dried over MgSO₄, filtered and evaporated under reduced pressure. The crude was then purified by normal-phase chromatography (CH₂Cl₂: MeOH, 95:5) to yield **CIR38-COOH** as a green solid (14 mg, 20% yield).

¹H NMR (500 MHz, MeOD) δ 8.87 (s, 1H), 8.70 (s, 1H), 8.32 (d, *J* = 7.9 Hz, 1H), 8.06 (t, *J* = 7.8 Hz, 1H), 7.53 – 7.48 (m, 1H), 7.45 – 7.36 (m, 4H), 7.34 (d, *J* = 2.5 Hz, 2H), 7.27 – 7.21 (m, 2H), 6.92 (dd, *J* = 14.1, 3.0 Hz, 2H), 6.37 (dd, *J* = 14.1, 6.2 Hz, 2H), 4.22 – 4.13 (m, 4H), 2.89 (s, 4H), 2.31 (t, *J* = 7.3 Hz, 3H), 2.22 – 2.11 (m, 2H), 1.91 – 1.82 (m, 4H), 1.75 – 1.67 (m, 3H), 1.35 (s, 6H), 1.28 (s, 6H), 1.05 (t, *J* = 7.4 Hz, 3H).

¹³C NMR (126 MHz, MeOD) δ 173.1, 172.9, 149.5, 148.9, 147.3, 142.1, 142.0, 141.4, 141.4, 141.1, 137.7, 128.6, 128.5, 128.5, 126.5, 126.5, 125.4, 125.4, 122.1, 111.2, 111.1, 101.6, 101.5, 49.1, 49.1, 45.4, 43.8, 26.8, 26.6, 26.0, 24.6, 24.1, 24.1, 20.6, 20.4, 10.2.

HRMS: *m/z* [M⁺] calcd. for C₄₆H₅₃O₂N₆: 721.4225; found: 721.4206.

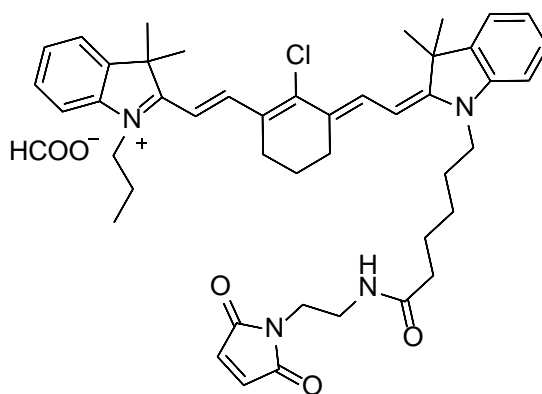


CIR38SE

CIR38SE. **CIR38-COOH** (9 mg, 0.01 mmol), *N*-hydroxysuccinimide (4 mg, 0.03 mmol), *N,N'*-dicyclohexylcarbodiimide (10 mg, 0.04 mmol) and DIPEA (4 μ L, 0.04 mmol) were dissolved in CHCl_3 (1.5 mL) with a catalytic amount of DMAP. The reaction was stirred at r.t. for 2 h. The reaction crude was purified by preparative TLC (CH_2Cl_2 : MeOH, 95:5) to yield **CIR38SE** as a green solid (7 mg, 81% yield).

^1H NMR (500 MHz, MeOD) δ 8.86 (s, 1H), 8.67 (d, J = 4.6 Hz, 1H), 8.31 (d, J = 8.0 Hz, 1H), 8.06 (td, J = 7.8, 1.8 Hz, 1H), 7.52 – 7.48 (m, 1H), 7.43 – 7.37 (m, 4H), 7.33 (d, J = 10.6 Hz, 2H), 7.24 (t, J = 7.9 Hz, 2H), 6.92 (d, J = 14.2 Hz, 2H), 6.37 (dd, J = 14.1, 4.1 Hz, 2H), 4.23 – 4.11 (m, 4H), 2.90 – 2.85 (m, 4H) 2.86 (s, 4H), 1.92 – 1.81 (m, 5H), 1.64 – 1.53 (m, 2H), 1.35 (s, 6H), 1.27 (s, 6H), 1.05 (t, J = 7.4 Hz, 3H), 0.95 – 0.84 (m, 5H). **^{13}C NMR** (126 MHz, MeOD) δ 173.6, 173.0, 171.3, 170.4, 149.6, 148.9, 148.0, 147.3, 145.5, 141.9, 141.1, 137.8, 129.4, 128.5, 126.5, 125.4, 123.7, 122.1, 120.4, 114.5, 111.1, 111.1, 107.4, 104.7, 101.6, 100.6, 96.1, 53.6, 45.4, 45.3, 43.9, 43.8, 31.7, 30.5, 30.0, 29.3, 26.6, 25.5, 25.1, 24.9, 24.1, 23.9, 22.3, 20.6, 20.4, 13.0, 10.2.

HRMS: m/z [M^+] calcd. for $\text{C}_{50}\text{H}_{56}\text{N}_7\text{O}_4$: 818.4388; found: 818.4453.



IR780M

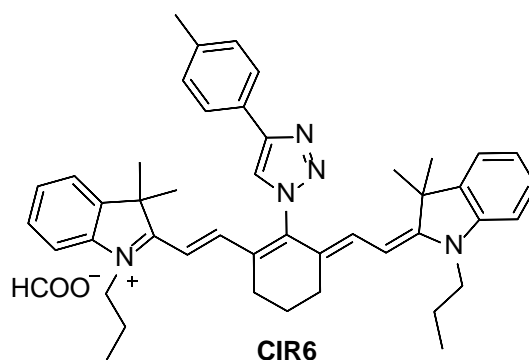
IR780M. To a solution of 3*H*-indolium,1-(5-carboxypentyl)-2,3,3-trimethylbromide (50 mg, 0.14 mmol) and 1-cyano-2-ethoxy-2-oxoethylidenaminoxy) dimethylaminomorpholino-carbeniumhexafluorophosphate (COMU) (90 mg, 0.21 mmol) dissolved in ACN (0.4 mL), DIPEA (37 μ L, 0.21 mmol) was added. The mixture was stirred at r.t. for 10 min. Next, 2-maleimidoethylamine (36 mg, 0.21 mmol) and DIPEA (37 μ L, 0.21 mmol) were added in ACN (0.2 mL) and the mixture was stirred at r.t. for 2 h. Then, H₂O (20 mL) was added to the reaction mixture which was extracted with CH₂Cl₂ (3 \times 20 mL). The organic extracts were dried over MgSO₄, filtered and evaporated under reduced pressure. The resulting crude was used in the next step without any purification. To a solution of AcONa (65 mg, 0.80 mmol) in AcOH (5 mL), 2-chloro-3-(hydroxymethylene)-1-cyclohexene-1-carboxaldehyde (21 mg, 0.14 mmol) and 3*H*-indolium,2,3,3-trimethyl-1-propyl iodide (37 mg, 0.14 mmol) were added. The resulting solution was stirred at 130 °C under reflux for 2 h. Next, 1-(6-((2-(2,5-dioxo-2,5-dihydro-1H-pyrrol-1-yl)ethyl)amino)-6-oxohexyl)-2,3,3-trimethyl-3*H*-indol-1-ium bromide (56 mg, 0.14 mmol) was added to the reaction mixture, which was stirred for 2 h at 130 °C. The reaction was then cooled to r.t. and solvents were evaporated under reduced pressure. The resulting crude was then purified by semi-preparative HPLC to isolate **IR780-M** as a green solid (2 mg).

¹H NMR (500 MHz, MeOD) δ 8.50 – 8.43 (m, 1H), 7.55 (ddd, J = 7.6, 3.7, 1.1 Hz, 2H), 7.46 (td, J = 7.7, 1.2 Hz, 2H), 7.41 – 7.34 (m, 2H), 7.32 (tdd, J = 7.5, 3.0, 0.9 Hz, 2H), 6.81 (s, 2H), 6.32 (d, J = 14.1 Hz, 1H), 5.51 (s, 2H), 4.25 – 4.13 (m, 2H), 4.12 – 4.03 (m, 2H), 3.89 – 3.79 (m, 4H), 3.60 –

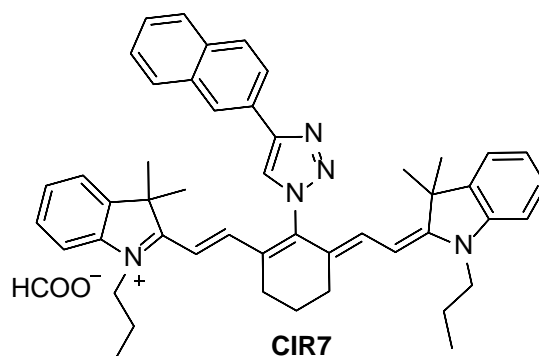
3.54 (m, 4H), 2.80 – 2.69 (m, 2H), 2.37 (t, $J = 7.4$ Hz, 2H), 1.76 (s, 6H), 1.76 (s, 6H), 1.69 – 1.59 (m, 2H), 1.38 – 1.31 (m, 5H), 1.08 (t, $J = 7.4$ Hz, 3H), 0.98 – 0.88 (m, 2H).

HRMS: m/z [M^+] calcd. for $C_{45}H_{54}ClN_4O_3$: 733.3879; found: 733.3849.

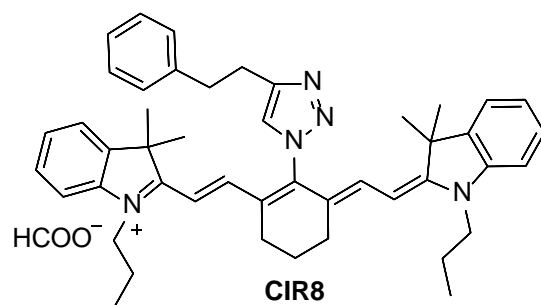
CIR library (representative subset)



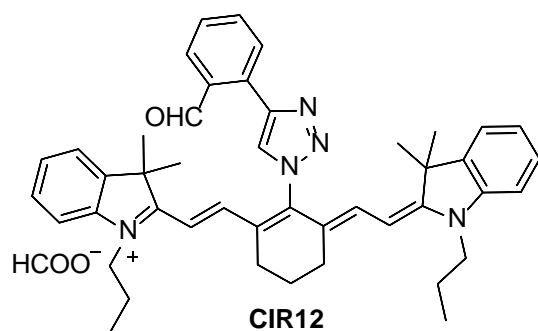
¹H NMR (500 MHz, MeOD) δ 8.81 (s, 1H), 7.89 (d, $J = 8.1$ Hz, 2H), 7.45 – 7.34 (m, 5H), 7.36 – 7.29 (m, 2H), 7.28 – 7.20 (m, 2H), 6.94 (d, $J = 14.2$ Hz, 3H), 6.36 (d, $J = 14.2$ Hz, 2H), 4.16 (t, $J = 7.3$ Hz, 2H), 2.91 – 2.83 (m, 2H), 2.45 (s, 3H), 1.87 (q, $J = 7.4$ Hz, 4H), 1.35 (s, 6H), 1.30 (s, 6H), 1.25 – 1.12 (m, 4H), 1.04 (t, $J = 7.4$ Hz, 6H), 1.01 – 0.93 (m, 2H). **¹³C NMR** (126 MHz, MeOD) δ 173.1, 148.2, 147.7, 142.1, 141.6, 141.1, 138.9, 129.5, 128.5, 126.6, 126.4, 125.5, 125.4, 124.5, 122.1, 111.1, 101.4, 49.1, 45.4, 26.6, 24.1, 20.6, 20.0, 10.2.



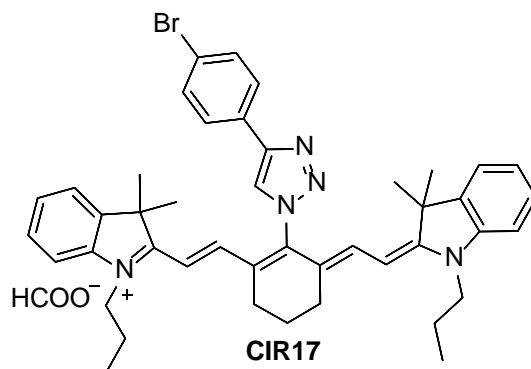
¹H NMR (500 MHz, MeOD) δ 9.01 (s, 1H), 8.55 (s, 1H), 8.12 (dd, $J = 8.5, 1.7$ Hz, 1H), 8.08 – 8.03 (m, 1H), 8.04 – 7.99 (m, 1H), 7.96 (dd, $J = 7.8, 1.9$ Hz, 1H), 7.63 – 7.55 (m, 2H), 7.44 – 7.35 (m, 4H), 7.32 (dt, $J = 8.0, 0.8$ Hz, 2H), 7.21 (td, $J = 7.5, 1.0$ Hz, 2H), 6.99 (d, $J = 14.1$ Hz, 2H), 6.38 (d, $J = 14.1$ Hz, 2H), 4.16 (t, $J = 7.4$ Hz, 2H), 2.89 (q, $J = 6.7$ Hz, 2H), 1.88 (q, $J = 7.4$ Hz, 4H), 1.37 (s, 6H), 1.30 (s, 6H), 1.24 – 1.15 (m, 4H), 1.05 (t, $J = 7.4$ Hz, 6H), 1.03 – 0.94 (m, 2H). **¹³C NMR** (126 MHz, MeOD) δ 173.1, 148.1, 147.7, 142.1, 141.6, 141.1, 133.7, 133.6, 128.8, 128.4, 127.9, 127.5, 126.8, 126.5, 126.4, 125.4, 125.1, 124.3, 123.2, 122.2, 111.1, 101.4, 49.1, 45.4, 26.6, 24.1, 20.6, 10.2.



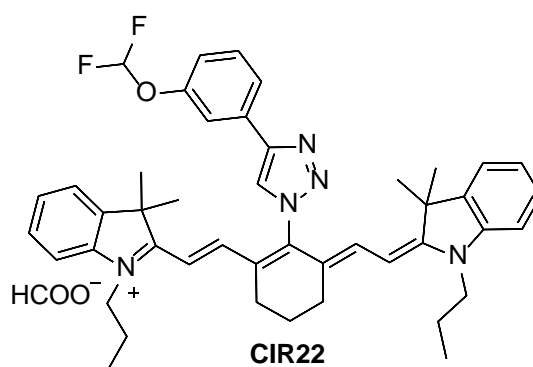
¹H NMR (500 MHz, MeOD) δ 8.19 (s, 1H), 7.50 – 7.42 (m, 3H), 7.44 – 7.38 (m, 4H), 7.40 – 7.31 (m, 4H), 7.32 – 7.25 (m, 2H), 6.80 (d, $J = 14.1$ Hz, 2H), 6.33 (d, $J = 14.2$ Hz, 2H), 4.15 (t, $J = 7.4$ Hz, 2H), 3.32 – 3.25 (m, 2H), 3.22 – 3.16 (m, 2H), 2.89 – 2.78 (m, 2H), 1.87 (q, $J = 7.4$ Hz, 4H), 1.34 (s, 6H), 1.22 (s, 6H), 1.05 (t, $J = 7.4$ Hz, 6H), 1.02 – 0.85 (m, 6H). **¹³C NMR** (126 MHz, MeOD) δ 173.0, 148.0, 142.1, 141.6, 141.1, 140.8, 128.5, 128.3, 128.3, 128.0, 128.0, 126.5, 126.1, 125.4, 123.9, 122.1, 111.1, 101.3, 49.1, 45.3, 35.3, 26.6, 24.0, 20.5, 10.2.



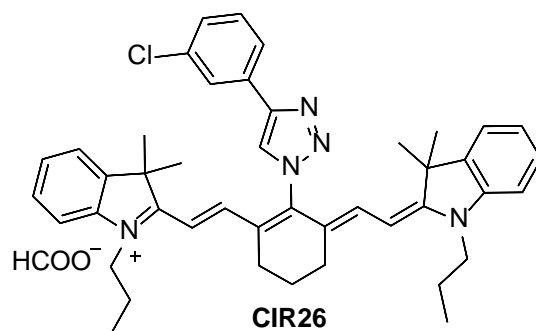
¹H NMR (500 MHz, MeOD) δ 10.57 (s, 1H), 8.90 (s, 1H), 8.66 (s, 1H), 8.21 – 8.10 (m, 2H), 7.96 – 7.83 (m, 2H), 7.73 (ddd, $J = 7.8, 1.4, 0.7$ Hz, 1H), 7.47 – 7.38 (m, 2H), 7.34 (dt, $J = 7.9, 0.8$ Hz, 2H), 7.27 (td, $J = 7.5, 0.9$ Hz, 2H), 6.94 (d, $J = 14.2$ Hz, 2H), 6.39 (d, $J = 14.1$ Hz, 2H), 4.26 – 4.09 (m, 2H), 2.98 – 2.83 (m, 2H), 1.89 (q, $J = 7.4$ Hz, 4H), 1.40 (s, 6H), 1.34 (s, 6H), 1.26 – 1.14 (m, 4H), 1.05 (t, $J = 7.4$ Hz, 6H), 1.03 – 0.88 (m, 2H). **¹³C NMR** (126 MHz, MeOD) δ 191.8, 173.0, 142.1, 141.4, 141.1, 134.0, 130.1, 129.4, 129.2, 128.5, 127.9, 126.6, 125.5, 122.1, 111.2, 101.6, 49.2, 45.4, 26.7, 24.1, 20.6, 10.2.



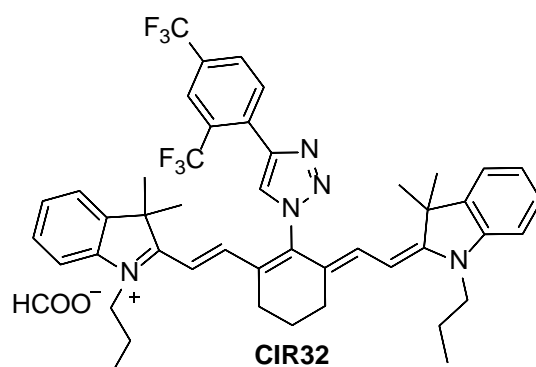
¹H NMR (500 MHz, MeOD) δ 8.90 (s, 1H), 7.95 (d, $J = 8.5$ Hz, 1H), 7.72 (d, $J = 8.6$ Hz, 2H), 7.46 – 7.37 (m, 5H), 7.36 – 7.30 (m, 2H), 7.26 (dd, $J = 7.4, 0.9$ Hz, 2H), 6.92 (d, $J = 14.2$ Hz, 2H), 6.36 (d, $J = 14.1$ Hz, 2H), 4.16 (t, $J = 7.3$ Hz, 2H), 2.93 – 2.82 (m, 2H), 1.87 (q, $J = 7.4$ Hz, 4H), 1.35 (s, 6H), 1.29 (s, 6H), 1.23 – 1.12 (m, 4H), 1.04 (t, $J = 7.4$ Hz, 6H), 1.00 – 0.86 (m, 2H). **¹³C NMR** (126 MHz, MeOD) δ 173.1, 147.5, 147.0, 142.1, 141.5, 141.1, 132.2, 128.5, 127.2, 126.4, 125.4, 122.2, 111.1, 101.4, 49.1, 45.4, 26.6, 24.1, 20.6, 10.2.



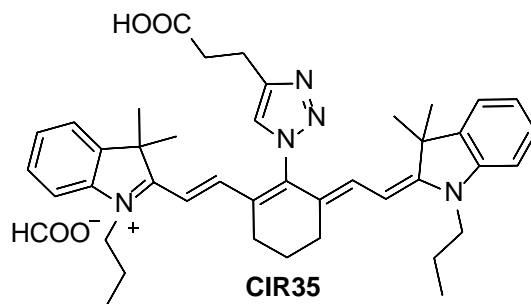
¹H NMR (500 MHz, MeOD) δ 8.95 (s, 1H), 7.91 – 7.80 (m, 2H), 7.59 (t, $J = 8.0$ Hz, 1H), 7.43 – 7.38 (m, 3H), 7.38 – 7.31 (m, 2H), 7.29 – 7.22 (m, 3H), 7.13 (s, 1H), 6.98 (s, 1H), 6.92 (d, $J = 14.1$ Hz, 2H), 6.37 (d, $J = 14.1$ Hz, 2H), 4.16 (t, $J = 7.4$ Hz, 2H), 2.92 – 2.84 (m, 2H), 1.87 (q, $J = 7.4$ Hz, 4H), 1.35 (s, 6H), 1.30 (s, 6H), 1.21 – 1.10 (m, 4H), 1.05 (t, $J = 7.4$ Hz, 6H), 0.99 – 0.94 (m, 2H). **¹³C NMR** (126 MHz, MeOD) δ 173.1, 152.2, 147.5, 147.0, 141.5, 131.5, 130.6, 128.5, 126.4, 125.4, 125.4, 122.3, 122.1, 119.1, 116.3, 116.2, 111.2, 101.5, 49.1, 45.4, 26.6, 26.6, 24.1, 20.6, 20.5, 10.2.



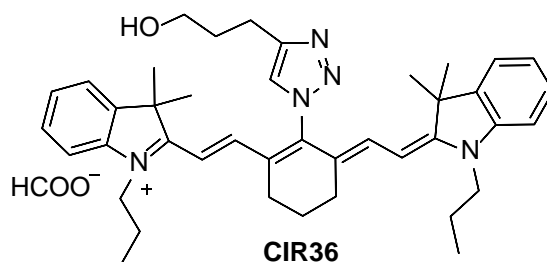
¹H NMR (500 MHz, MeOD) δ 8.94 (s, 1H), 8.56 (s, 1H), 8.08 (t, $J = 1.8$ Hz, 1H), 8.01 – 7.93 (m, 2H), 7.88 (d, $J = 8.0$ Hz, 1H), 7.59 – 7.52 (m, 1H), 7.49 (ddd, $J = 8.1, 2.1, 1.1$ Hz, 2H), 7.45 – 7.36 (m, 2H), 7.36 – 7.23 (m, 2H), 6.92 (d, $J = 14.3$ Hz, 2H), 6.36 (d, $J = 14.1$ Hz, 2H), 4.16 (t, $J = 7.3$ Hz, 2H), 2.87 (q, $J = 7.5, 7.0$ Hz, 2H), 1.87 (q, $J = 7.4$ Hz, 4H), 1.36 (s, 6H), 1.30 (s, 6H), 1.26 – 1.12 (m, 4H), 1.05 (t, $J = 7.4$ Hz, 6H), 1.02 – 0.91 (m, 2H). **¹³C NMR** (126 MHz, MeOD) δ 173.1, 142.1, 141.5, 141.1, 130.6, 128.5, 126.4, 125.5, 125.3, 123.7, 111.1, 101.4, 49.1, 45.4, 26.6, 24.1, 20.6, 10.2.



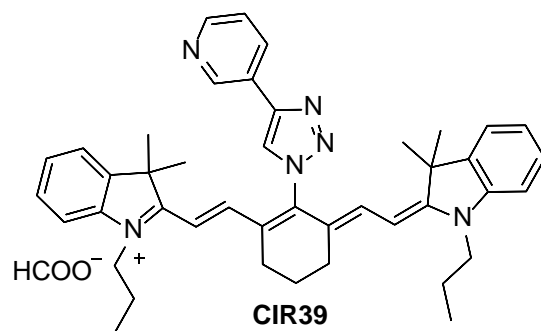
¹H NMR (500 MHz, MeOD) δ 9.19 (s, 1H), 8.72 – 8.62 (m, 2H), 8.10 (dt, $J = 1.9, 0.9$ Hz, 1H), 7.40 (dd, $J = 7.4, 1.3$ Hz, 4H), 7.39 – 7.31 (m, 2H), 7.25 (td, $J = 7.4, 0.9$ Hz, 2H), 6.92 (d, $J = 14.1$ Hz, 2H), 6.38 (d, $J = 14.1$ Hz, 2H), 4.17 (t, $J = 7.3$ Hz, 2H), 2.96 – 2.82 (m, 2H), 1.88 (q, $J = 7.4$ Hz, 4H), 1.36 (s, 6H), 1.29 (s, 6H), 1.21 – 1.18 (m, 4H), 1.05 (t, $J = 7.4$ Hz, 6H), 0.99 – 0.95 (m, 2H). **¹³C NMR** (126 MHz, MeOD) δ 173.1, 147.1, 145.1, 142.1, 141.3, 141.1, 132.4, 128.5, 126.4, 125.5, 122.2, 111.2, 101.6, 49.1, 45.4, 26.6, 26.4, 24.1, 20.6, 10.2.



¹H NMR (500 MHz, MeOD) δ 8.21 (s, 1H), 7.47 (dd, $J = 7.6, 1.1$ Hz, 2H), 7.46 – 7.39 (m, 2H), 7.34 (d, $J = 7.9$ Hz, 2H), 7.28 (td, $J = 7.5, 0.9$ Hz, 2H), 6.80 (d, $J = 14.1$ Hz, 2H), 6.33 (d, $J = 14.1$ Hz, 2H), 4.15 (t, $J = 7.3$ Hz, 2H), 3.23 (t, $J = 7.1$ Hz, 2H), 2.89 – 2.78 (m, 4H), 2.10 – 2.06 (m, 4H), 1.87 (q, $J = 7.4$ Hz, 4H), 1.37 (s, 6H), 1.35 (s, 6H), 1.05 (t, $J = 7.4$ Hz, 6H), 1.04 – 0.99 (m, 2H). **¹³C NMR** (126 MHz, MeOD) δ 173.0, 147.8, 147.6, 142.1, 141.6, 141.2, 128.5, 126.5, 126.0, 125.4, 122.1, 111.1, 101.3, 49.1, 45.3, 33.8, 26.9, 26.6, 24.0, 20.6, 20.6, 20.4, 10.2.



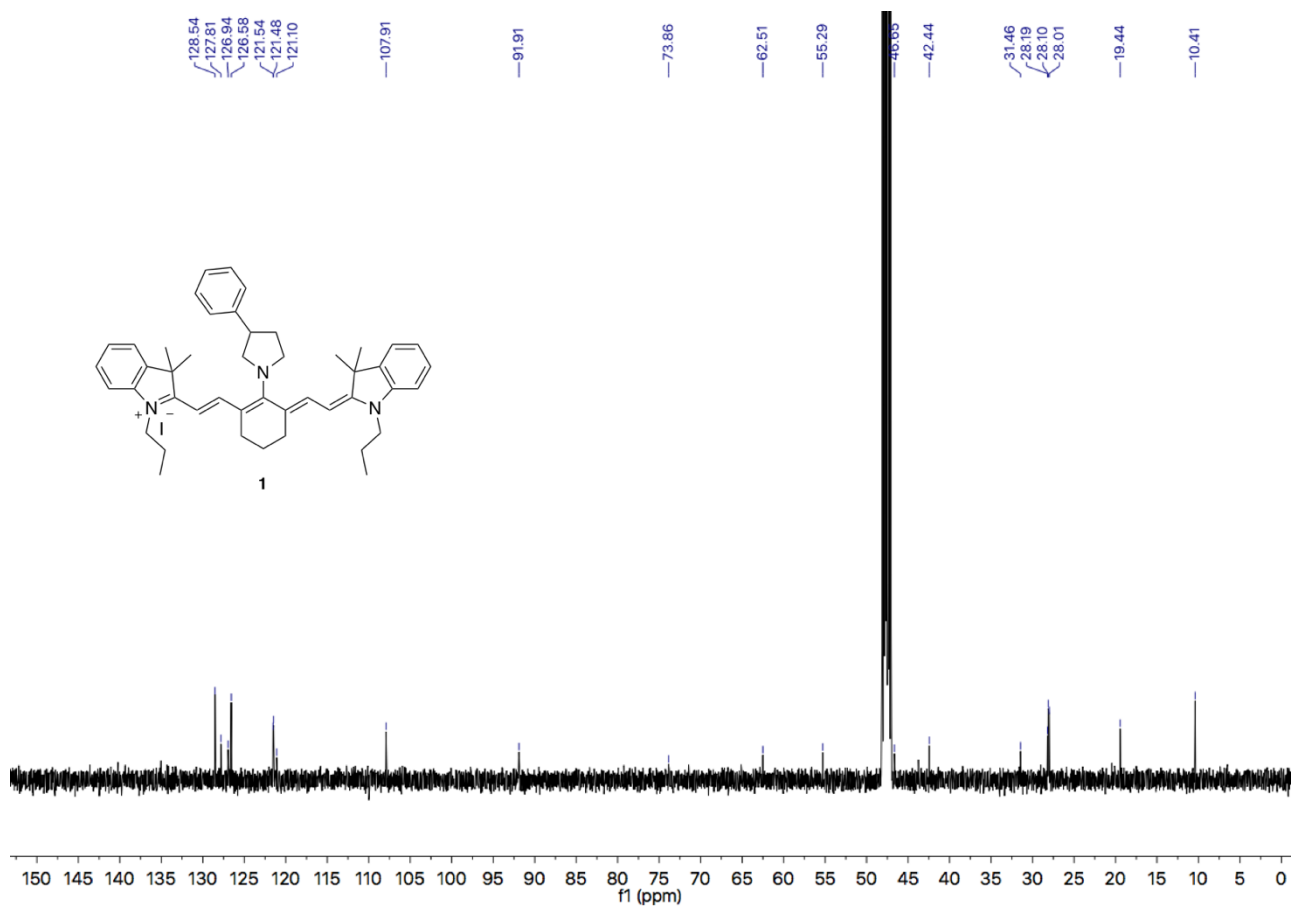
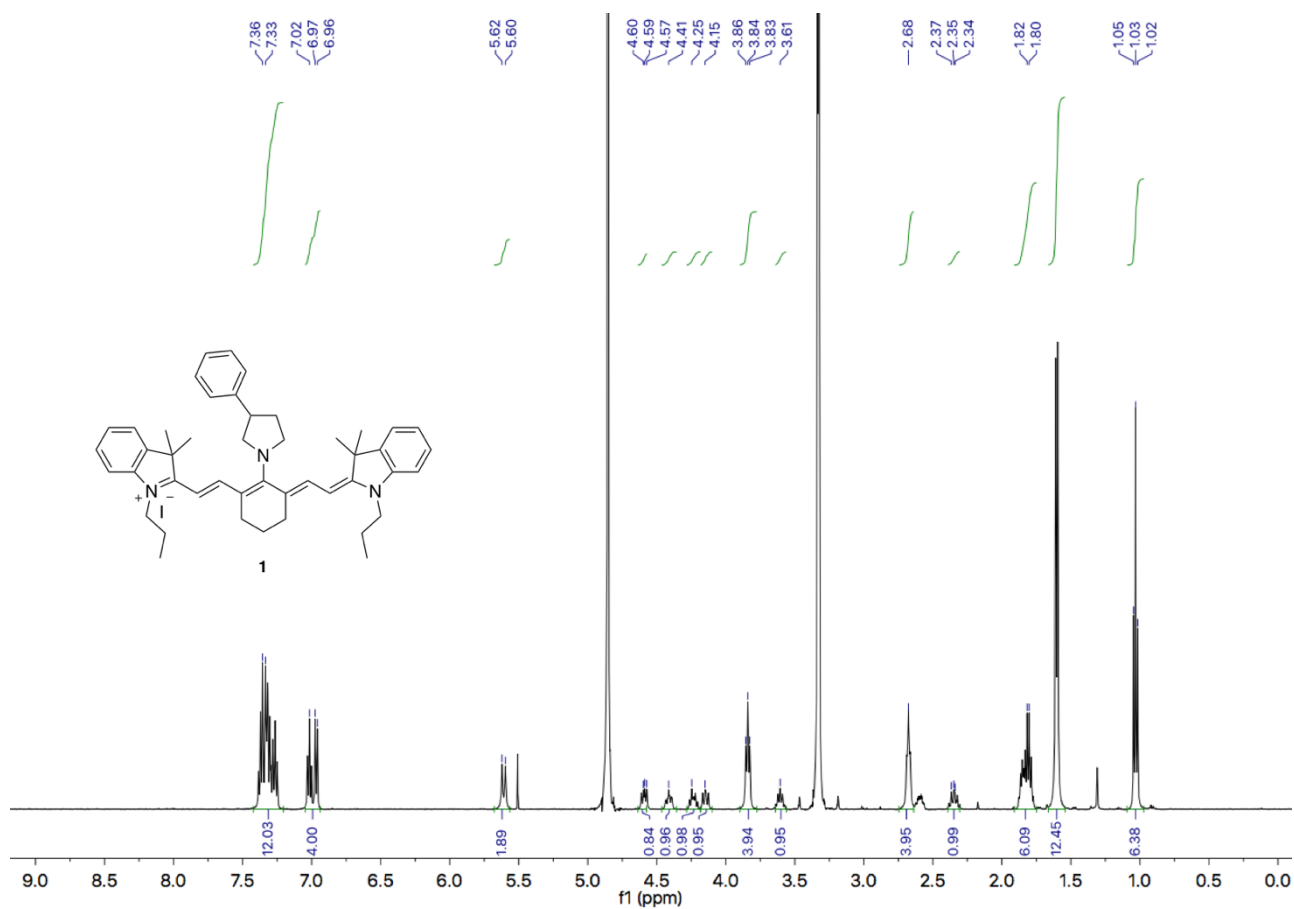
¹H NMR (500 MHz, MeOD) δ 8.20 (s, 1H), 7.91 (s, 1H), 7.44 (ddd, $J = 20.8, 7.6, 1.2$ Hz, 3H), 7.34 (d, $J = 8.0$ Hz, 2H), 7.28 (td, $J = 7.5, 0.9$ Hz, 2H), 6.82 (d, $J = 17.5$ Hz, 2H), 6.34 (d, $J = 14.1$ Hz, 2H), 4.29 – 4.18 (m, 1H), 4.15 (t, $J = 7.3$ Hz, 2H), 3.05 (d, $J = 6.2$ Hz, 2H), 2.83 (q, $J = 6.5, 5.4$ Hz, 4H), 1.88 (q, $J = 7.4$ Hz, 4H), 1.39 (s, 6H), 1.37 (s, 6H), 1.29 – 1.21 (m, 3H), 1.20 – 1.13 (m, 4H), 1.05 (t, $J = 7.4$ Hz, 6H), 1.02 – 0.84 (m, 2H). **¹³C NMR** (126 MHz, MeOD) δ 173.0, 147.8, 145.6, 142.1, 141.6, 141.2, 128.5, 126.7, 126.6, 125.4, 122.1, 111.1, 101.4, 66.5, 49.1, 48.1, 45.3, 34.4, 26.9, 26.6, 24.1, 22.3, 20.6, 10.2.



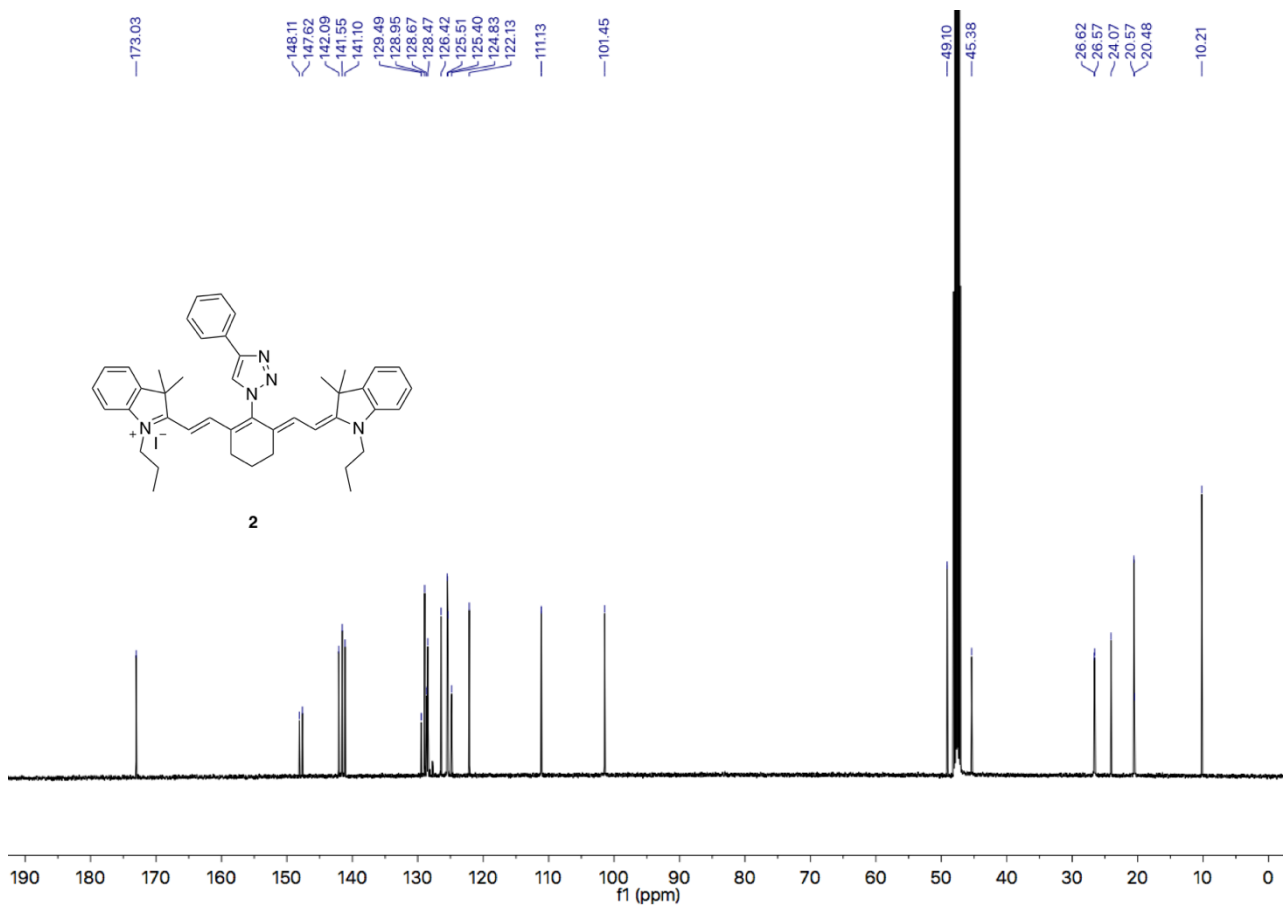
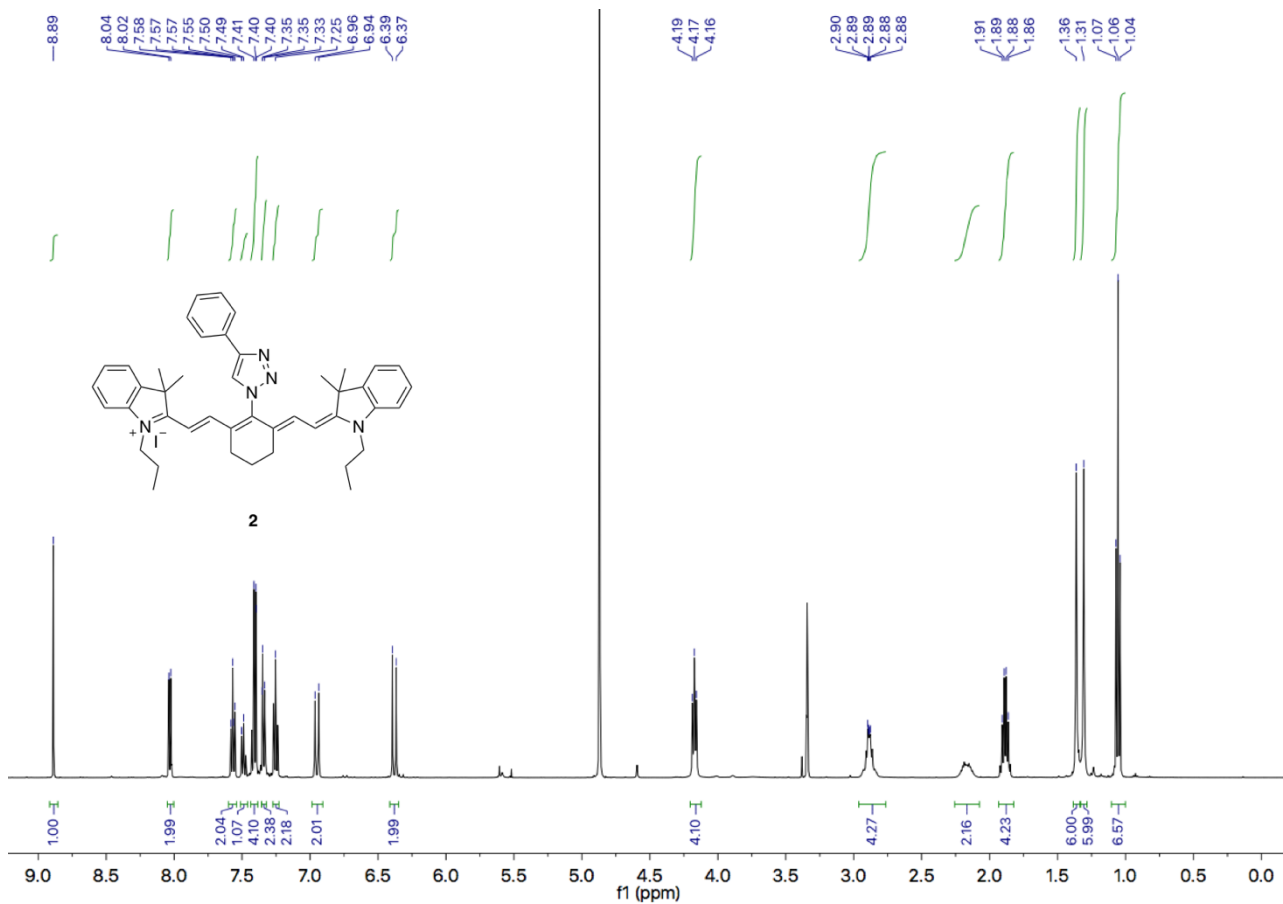
¹H NMR (500 MHz, MeOD) δ 9.04 (s, 1H), 8.66 (d, $J = 4.8$ Hz, 1H), 8.49 – 8.46 (m, 1H), 7.66 (dd, $J = 8.0, 4.8$ Hz, 1H), 7.45 – 7.38 (m, 4H), 7.36 – 7.32 (m, 2H), 7.25 (td, $J = 7.5, 0.9$ Hz, 2H), 6.91 (d, $J = 14.1$ Hz, 3H), 6.37 (d, $J = 14.1$ Hz, 2H), 4.16 (t, $J = 7.3$ Hz, 2H), 2.92 – 2.84 (m, 2H), 1.88 (q, $J = 7.4$ Hz, 4H), 1.36 (s, 6H), 1.29 (s, 6H), 1.24 – 1.13 (m, 4H), 1.05 (t, $J = 7.4$ Hz, 6H), 0.98 – 0.81 (m, 2H). **¹³C NMR** (126 MHz, MeOD) δ 173.1, 149.0, 147.3, 146.0, 144.7, 142.1, 141.4, 141.1, 133.7, 128.5, 126.4, 125.6, 125.5, 122.1, 111.2, 101.5, 49.1, 45.4, 26.6, 24.1, 20.6, 10.2.

NMR spectra

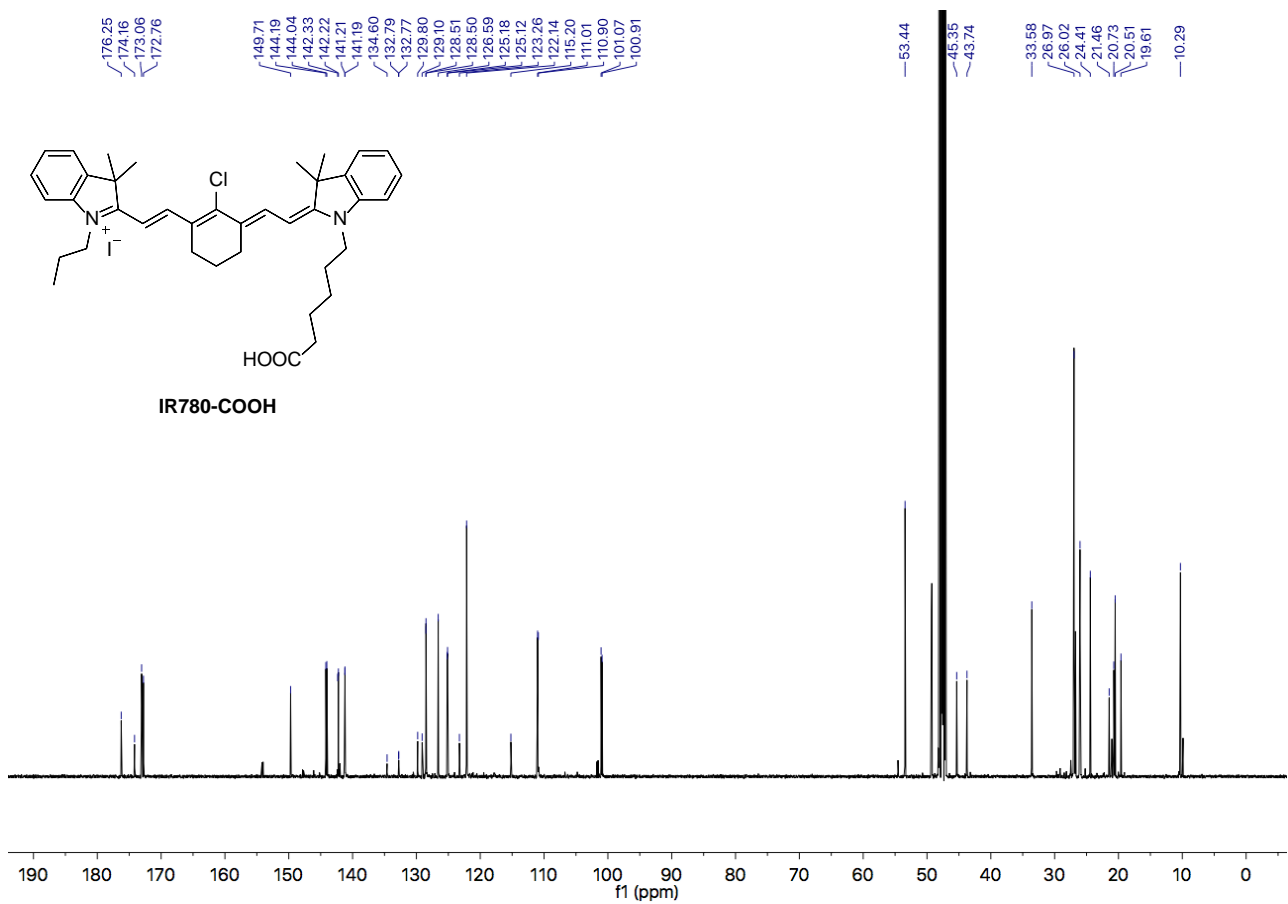
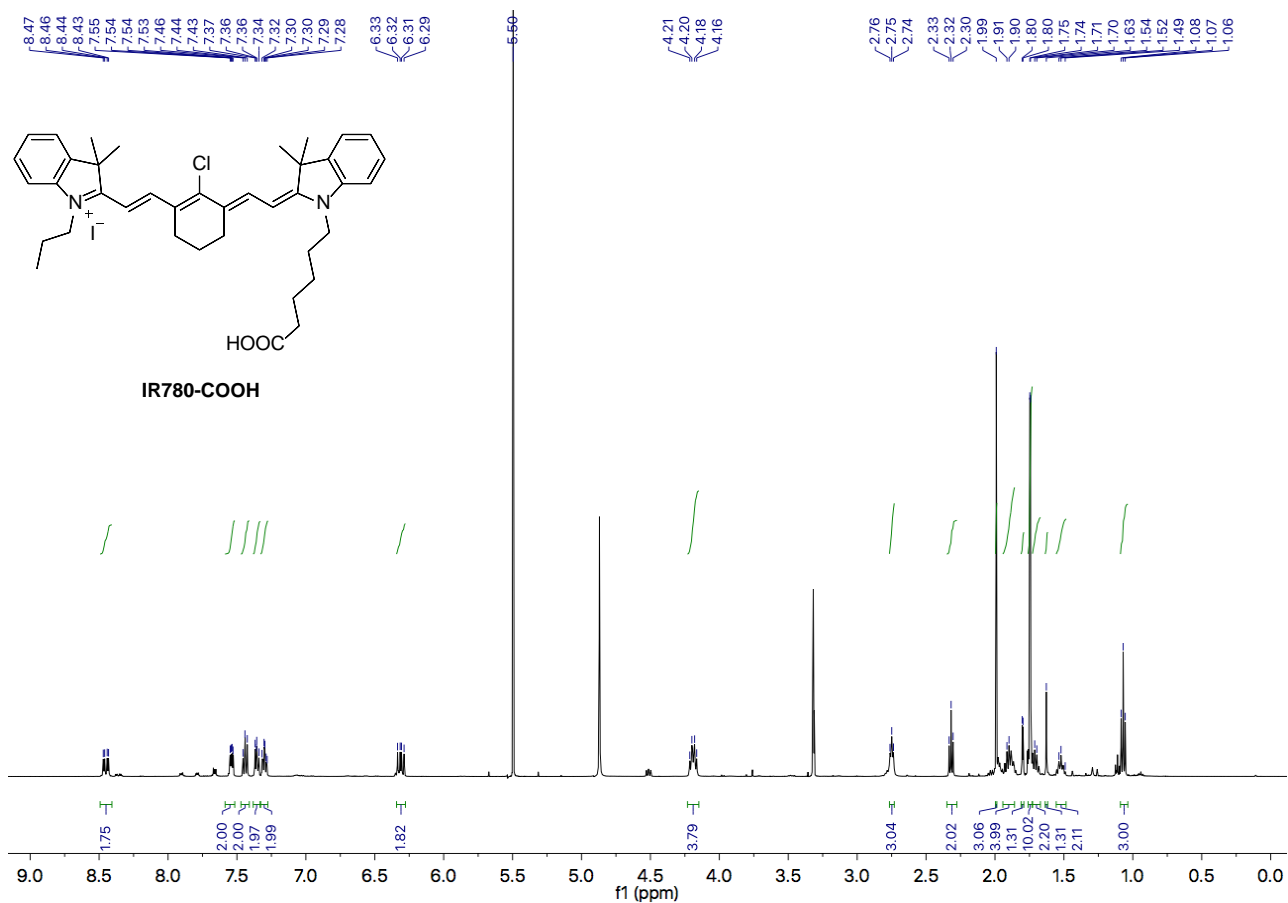
Compound 1



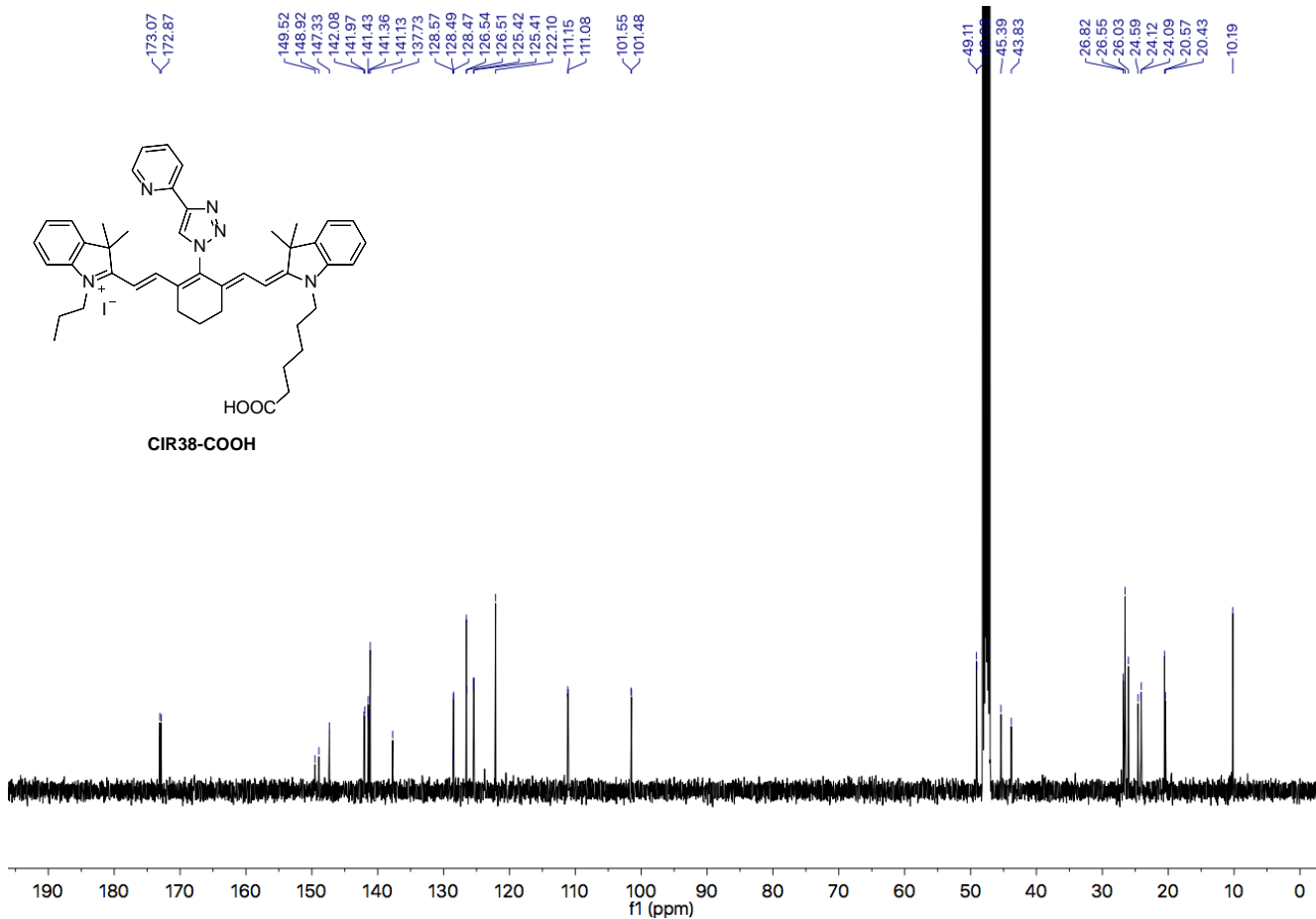
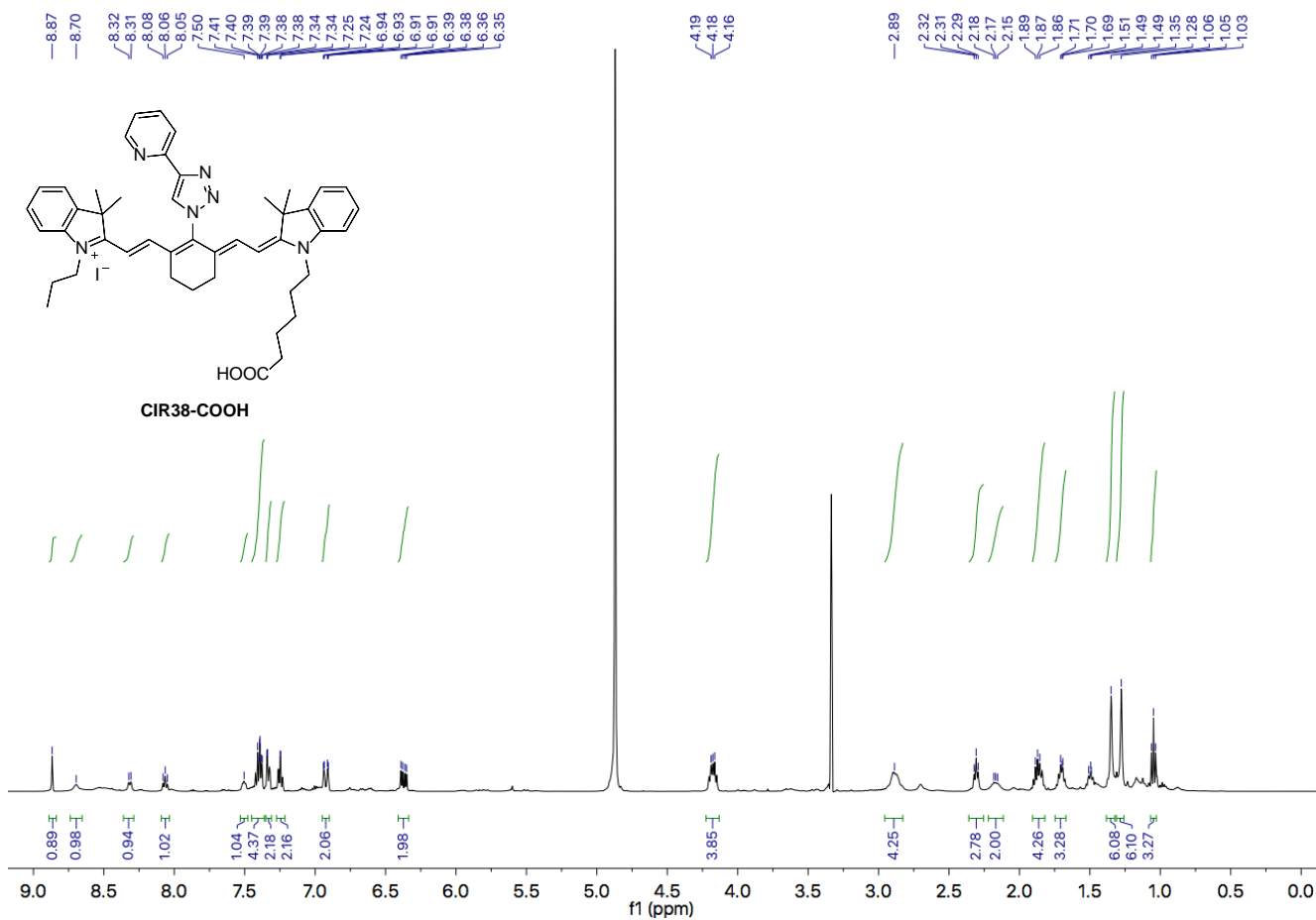
Compound 2



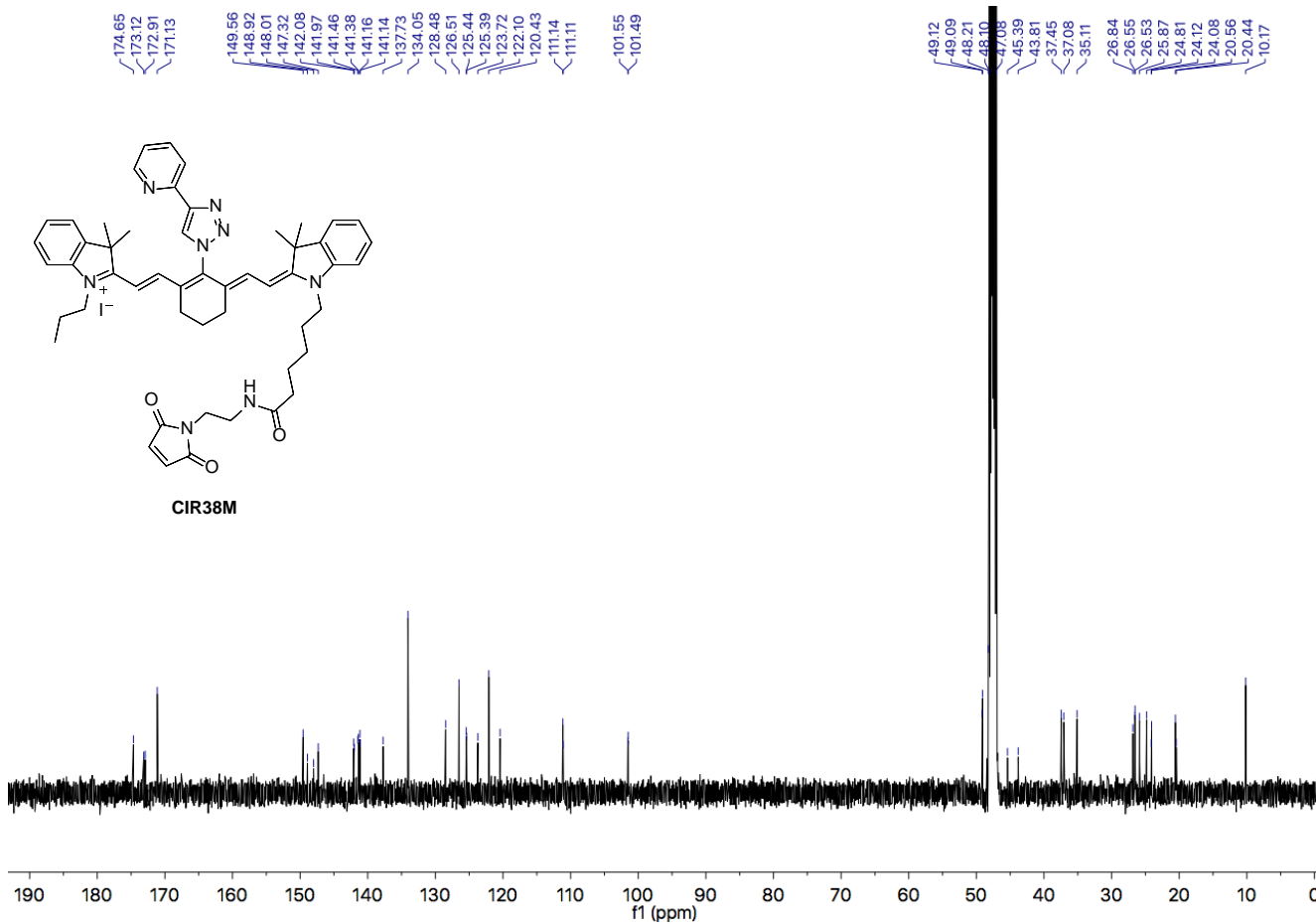
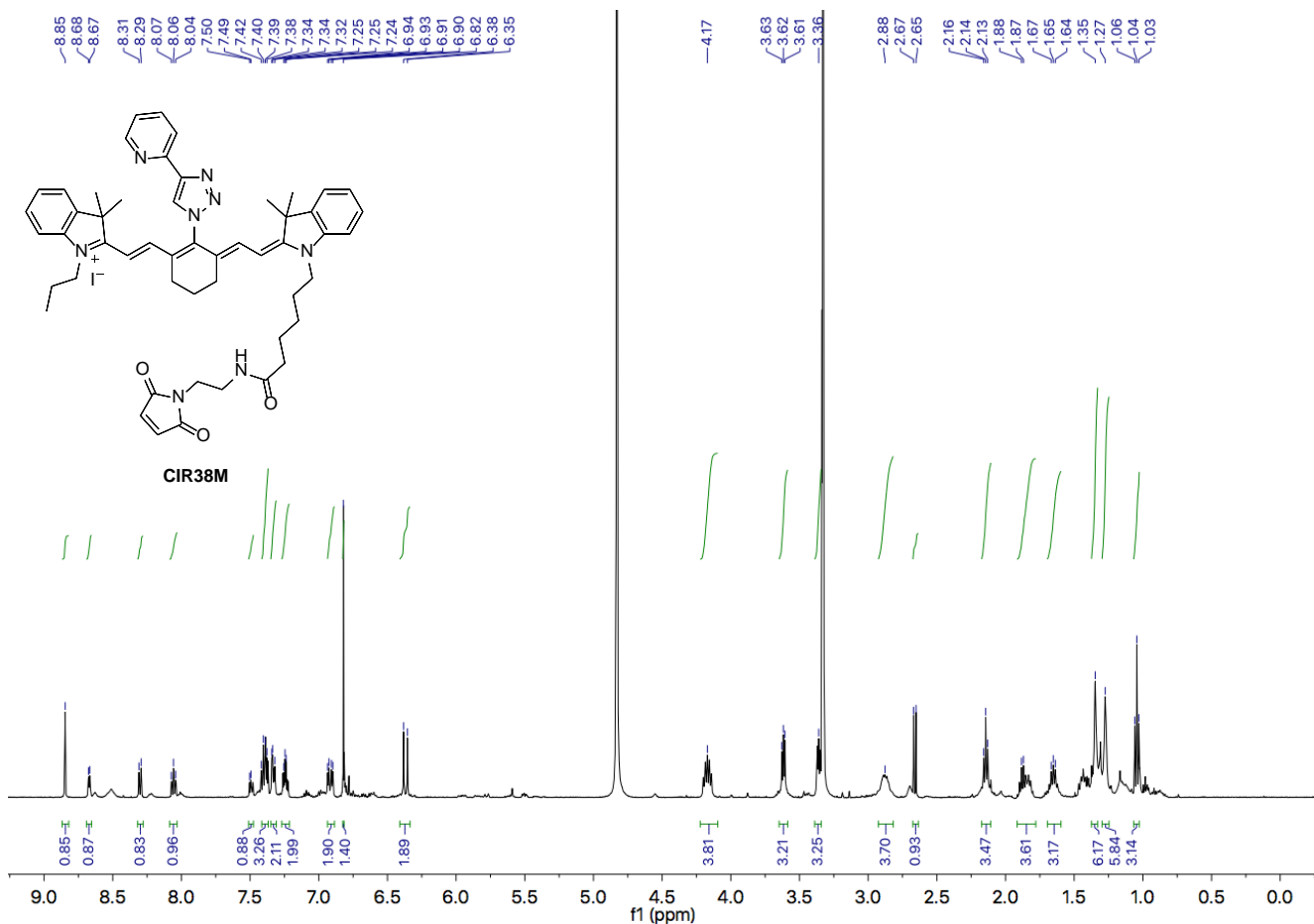
Compound IR780-COOH



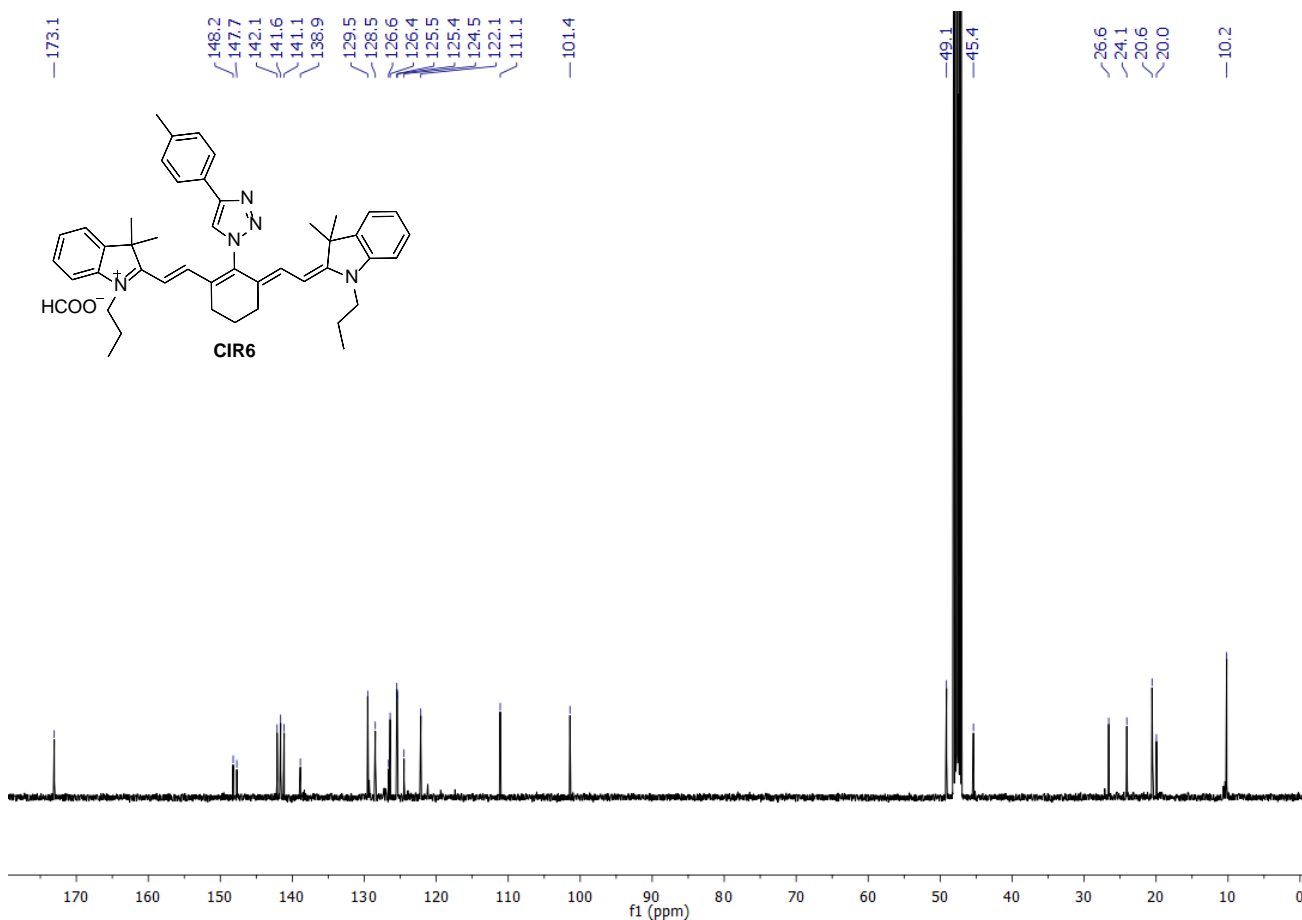
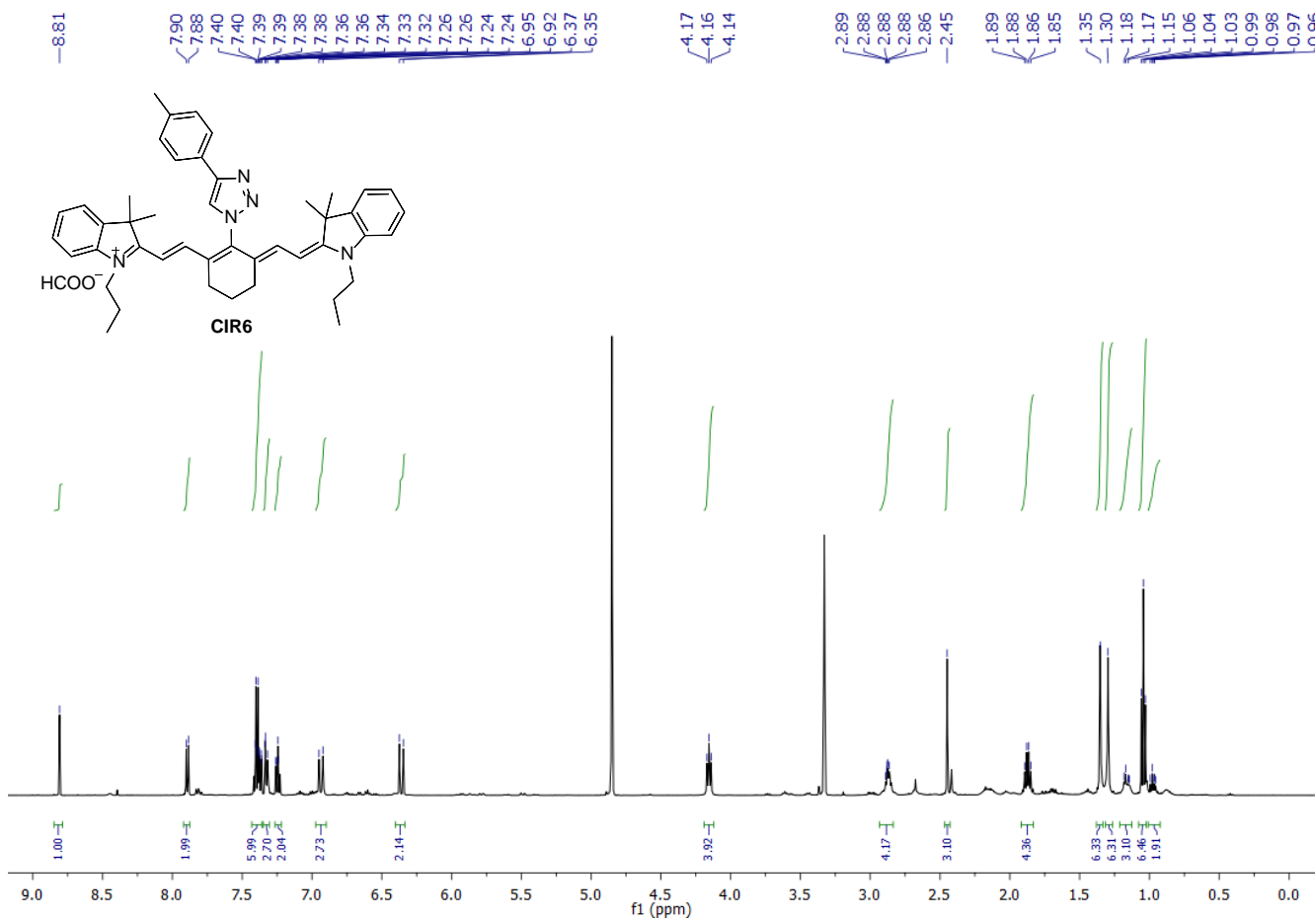
Compound CIR38-COOH

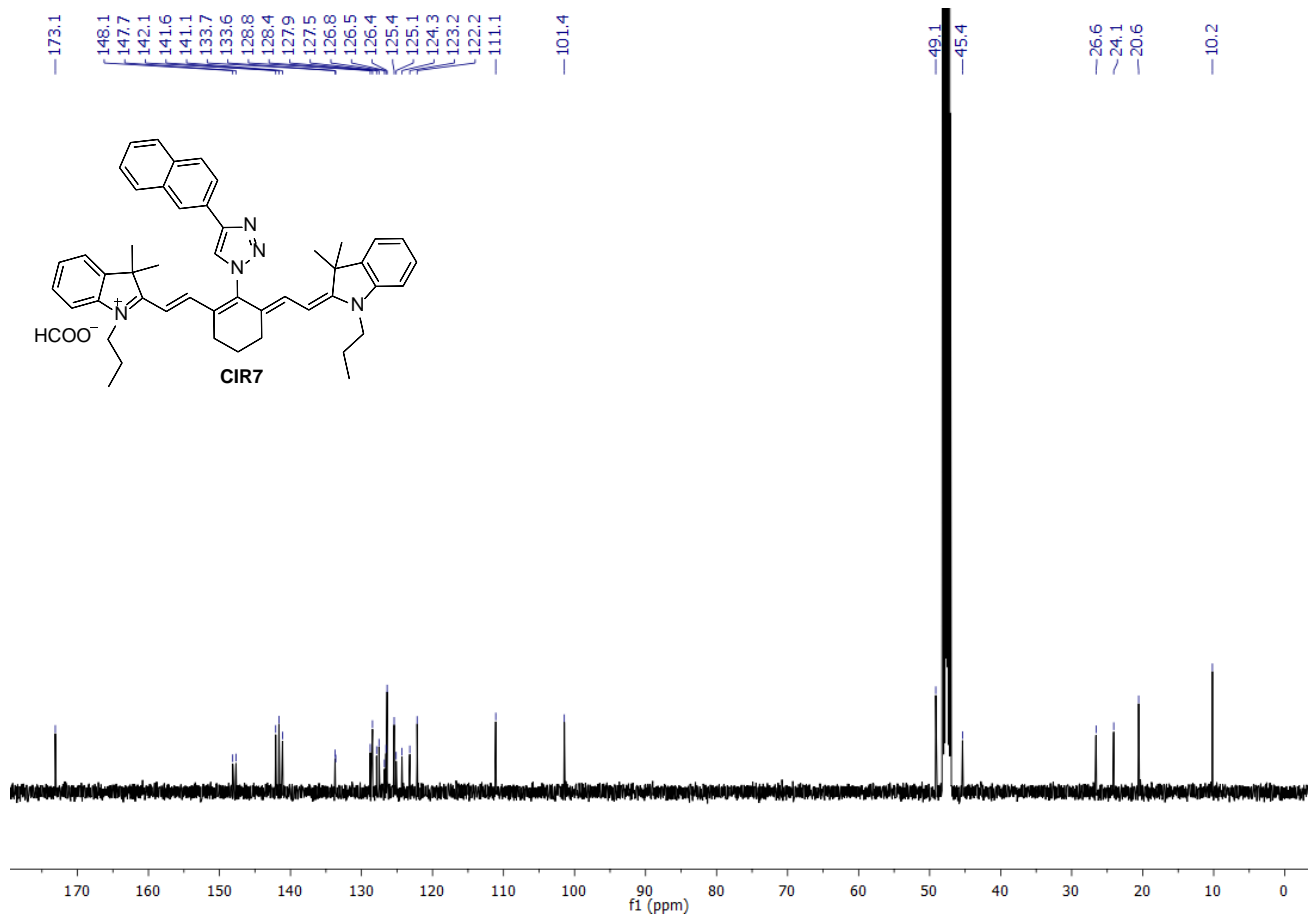
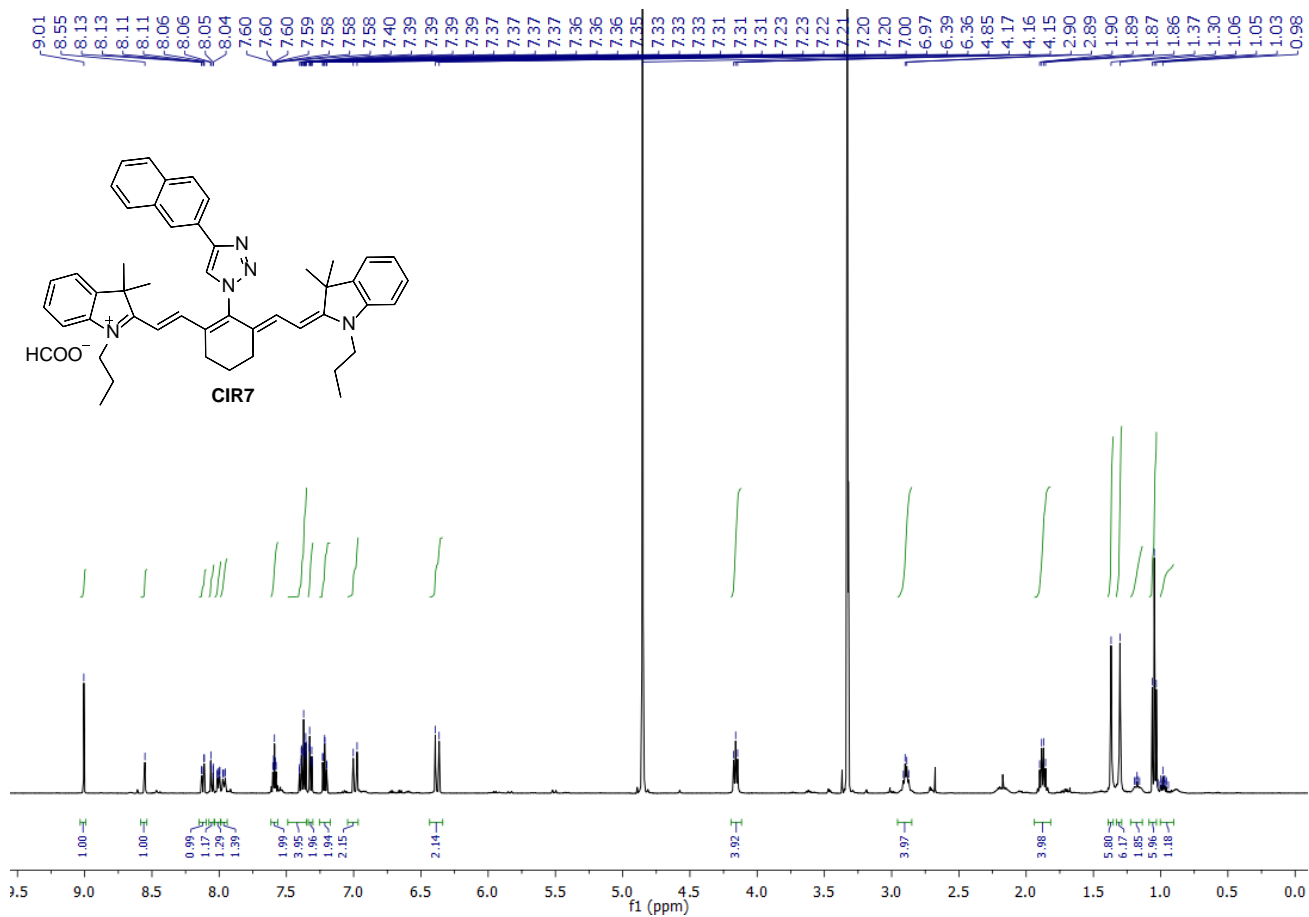


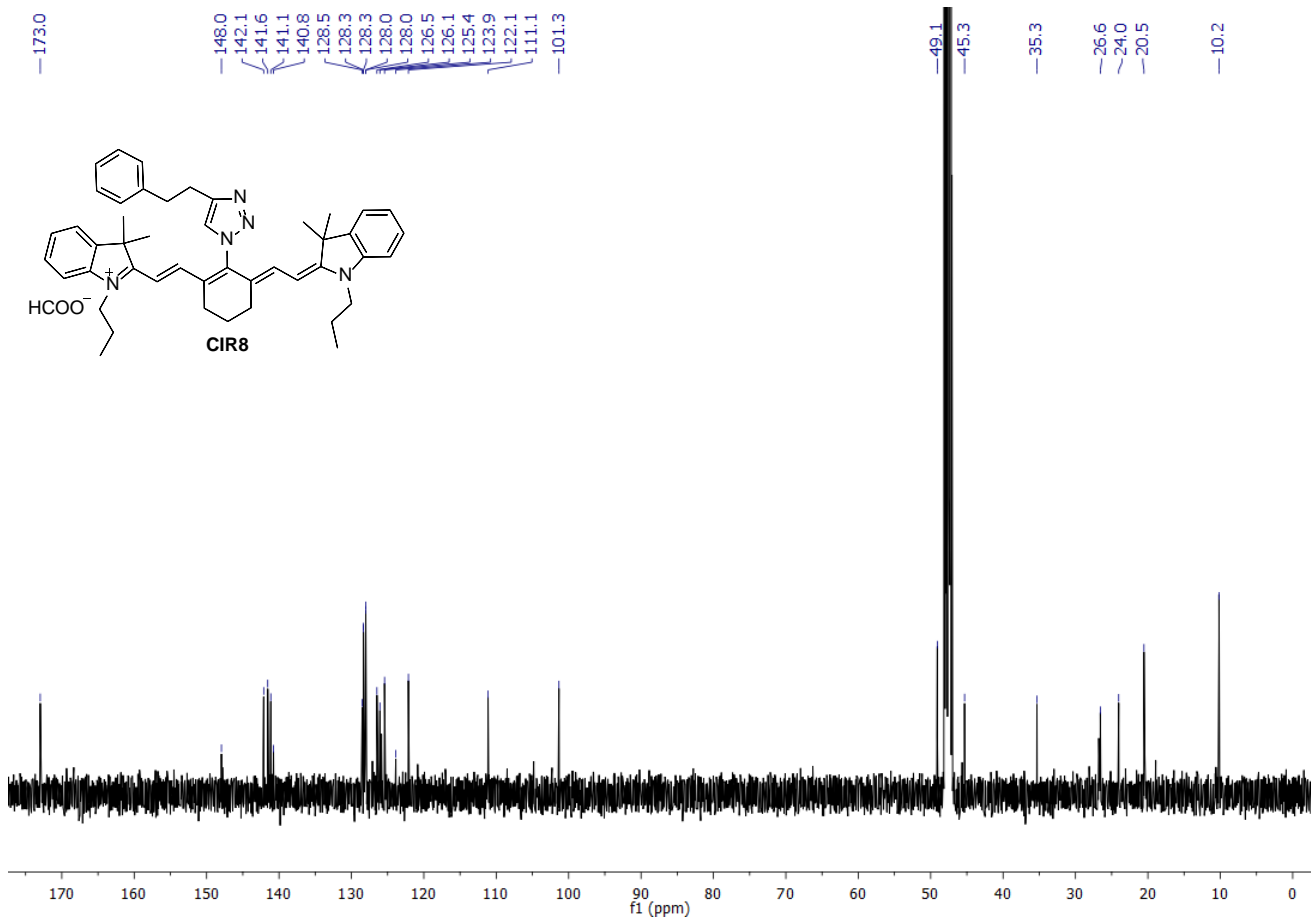
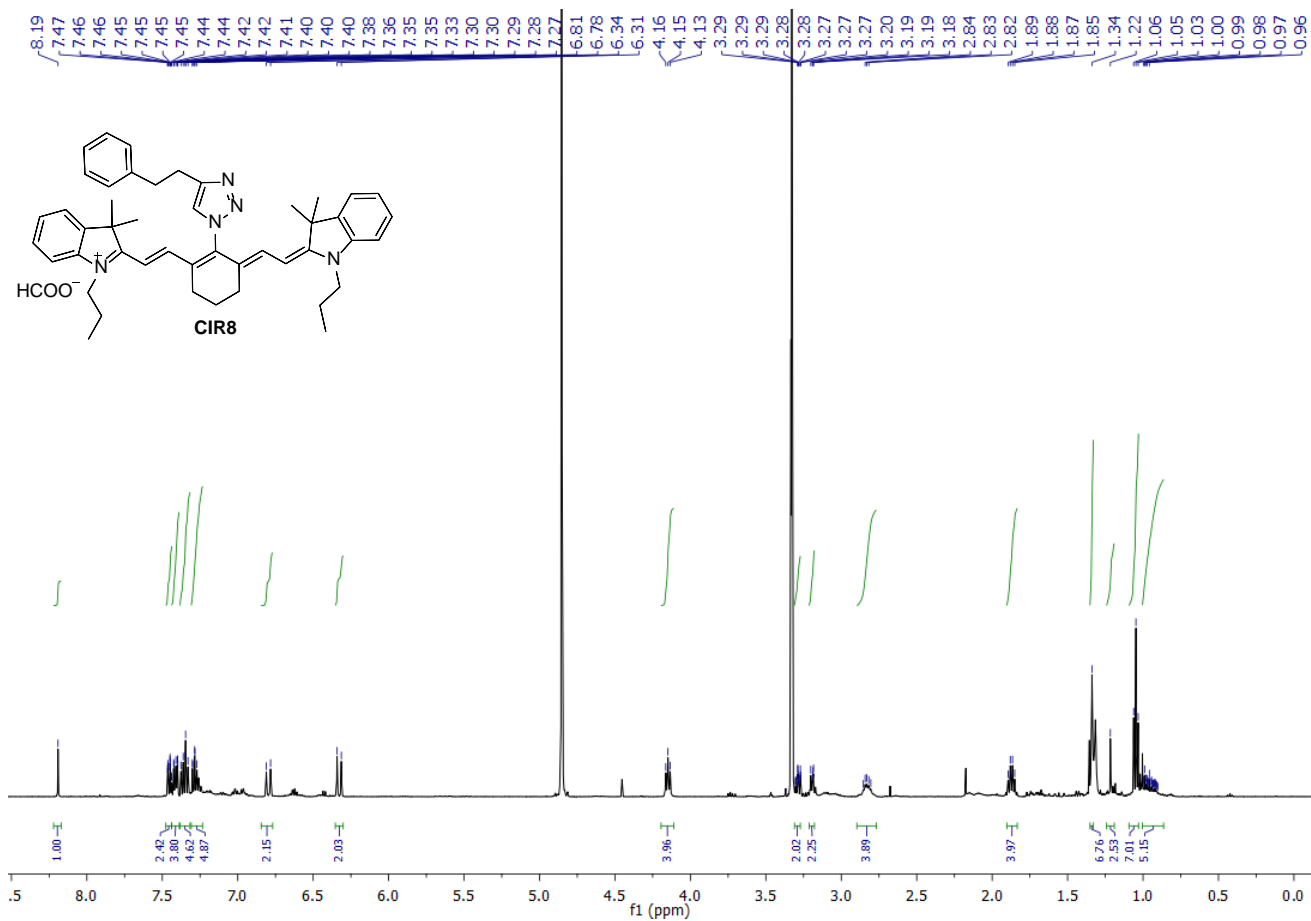
Compound CIR38M

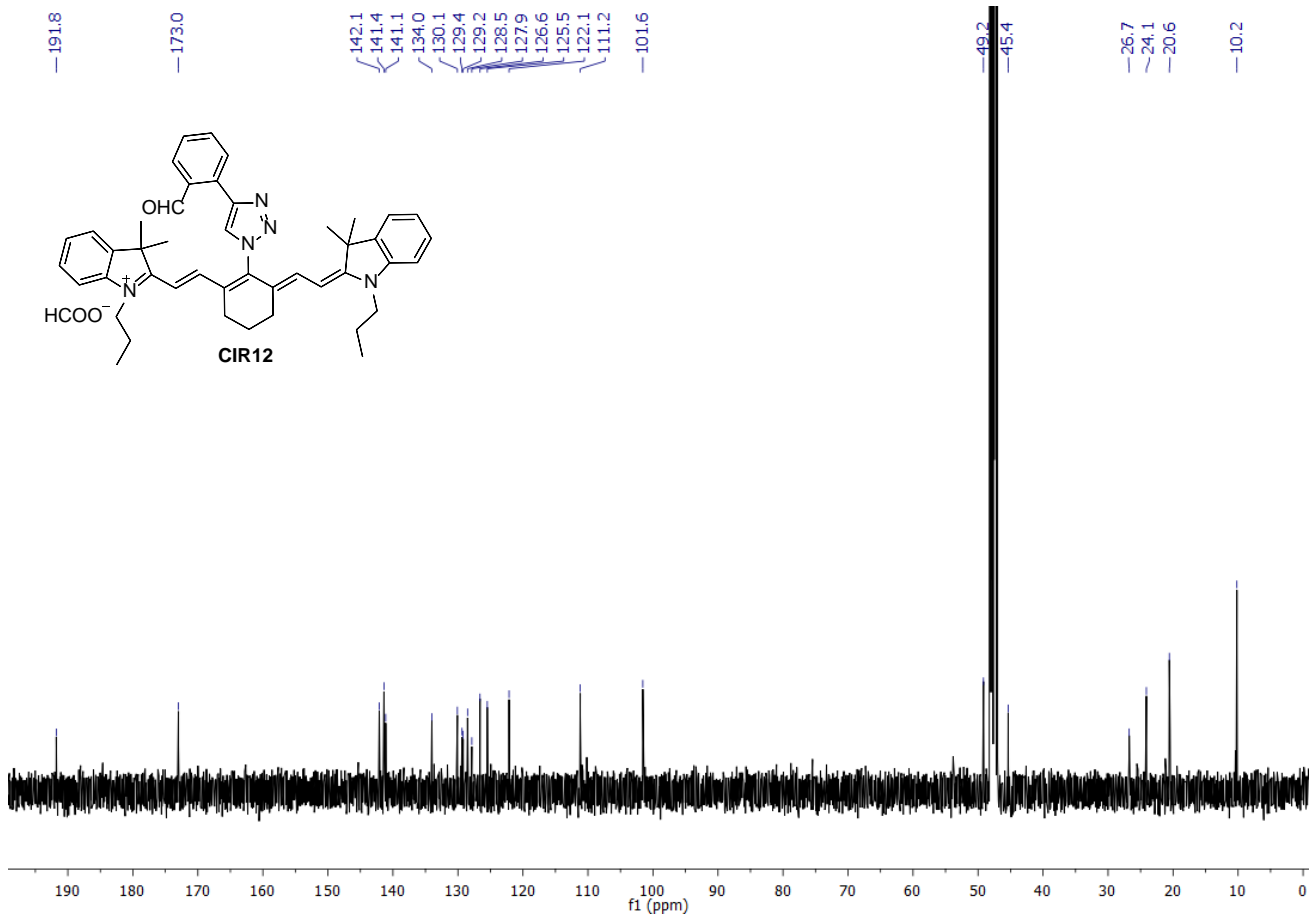
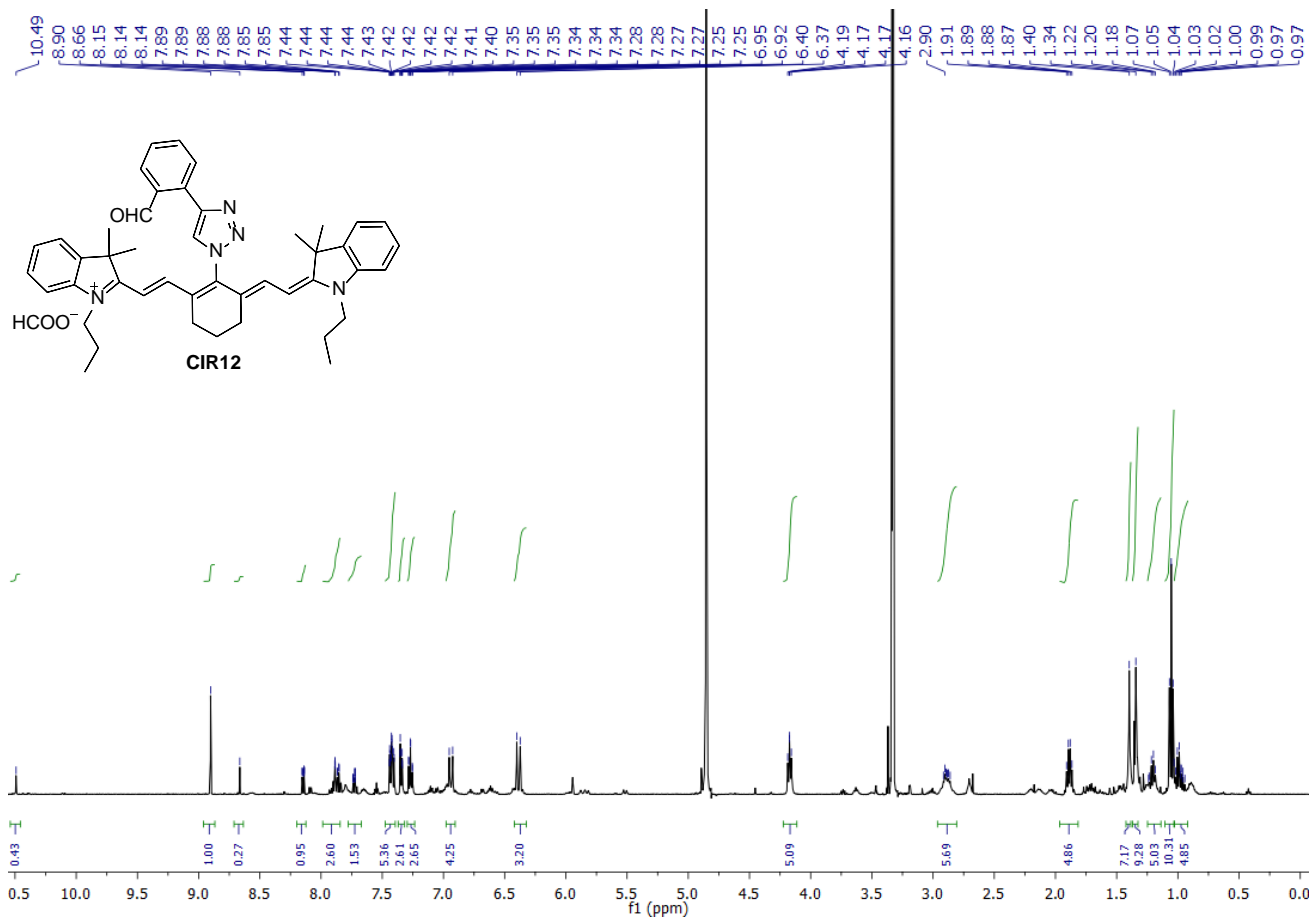


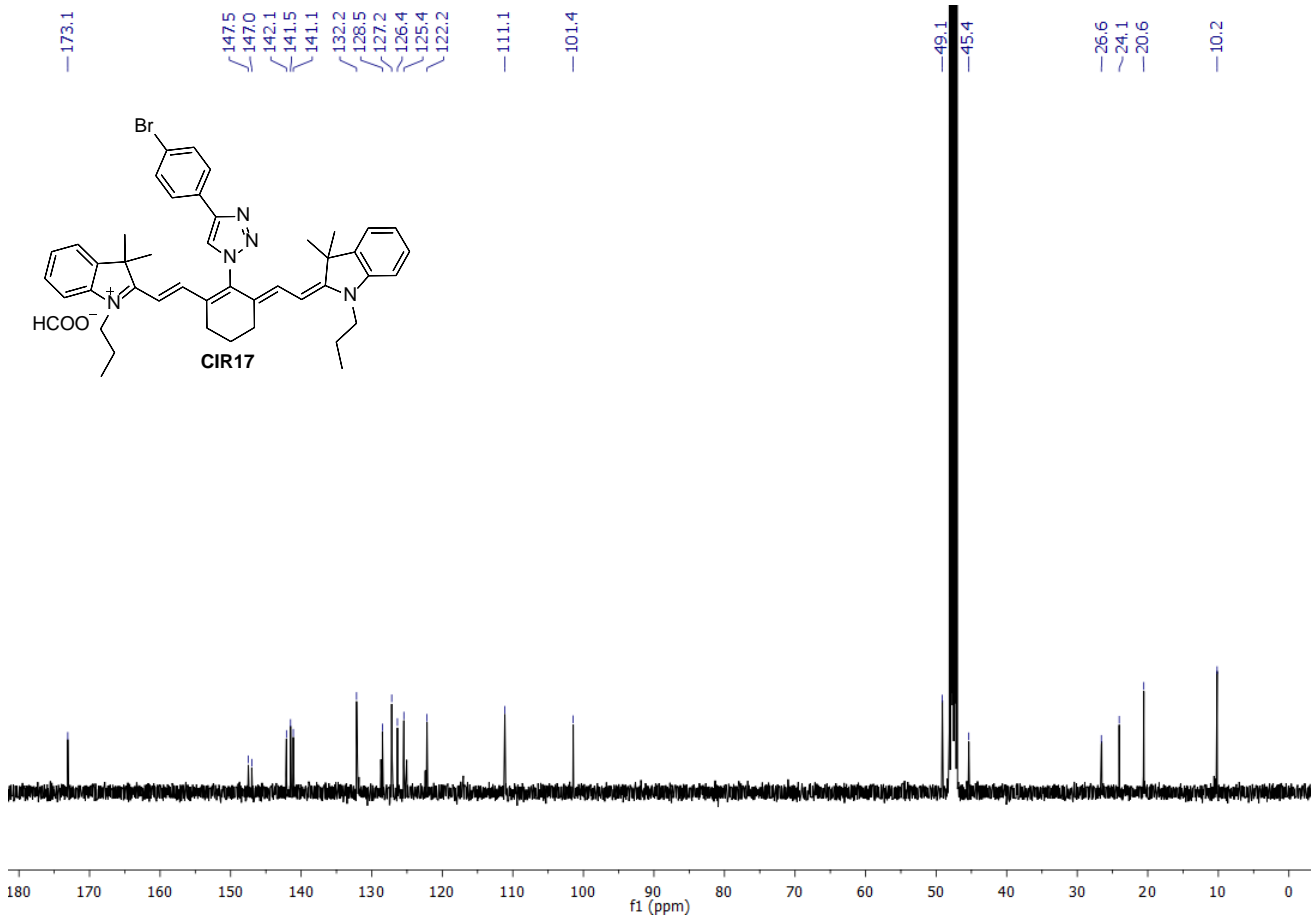
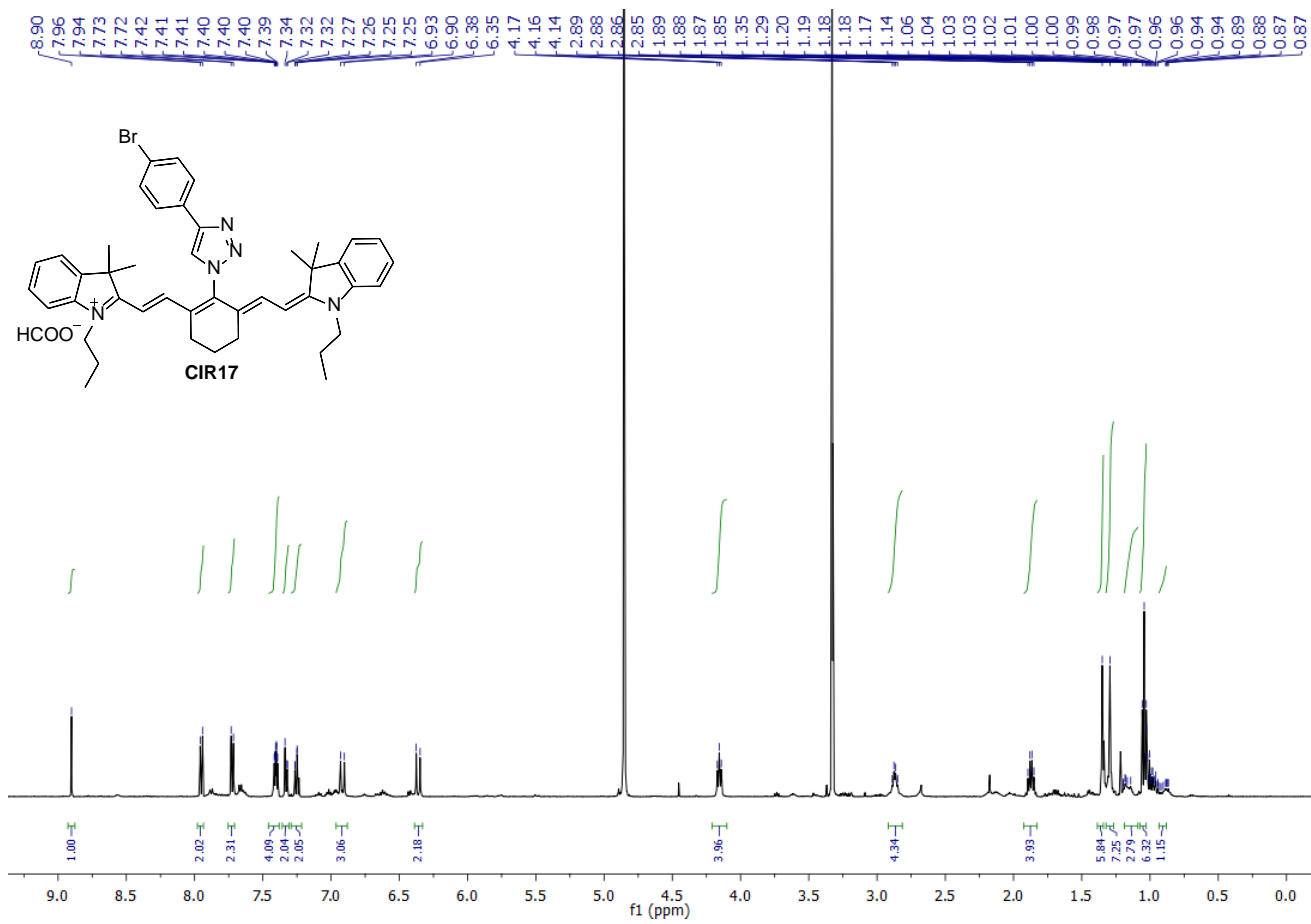
CIR library (representative subset)

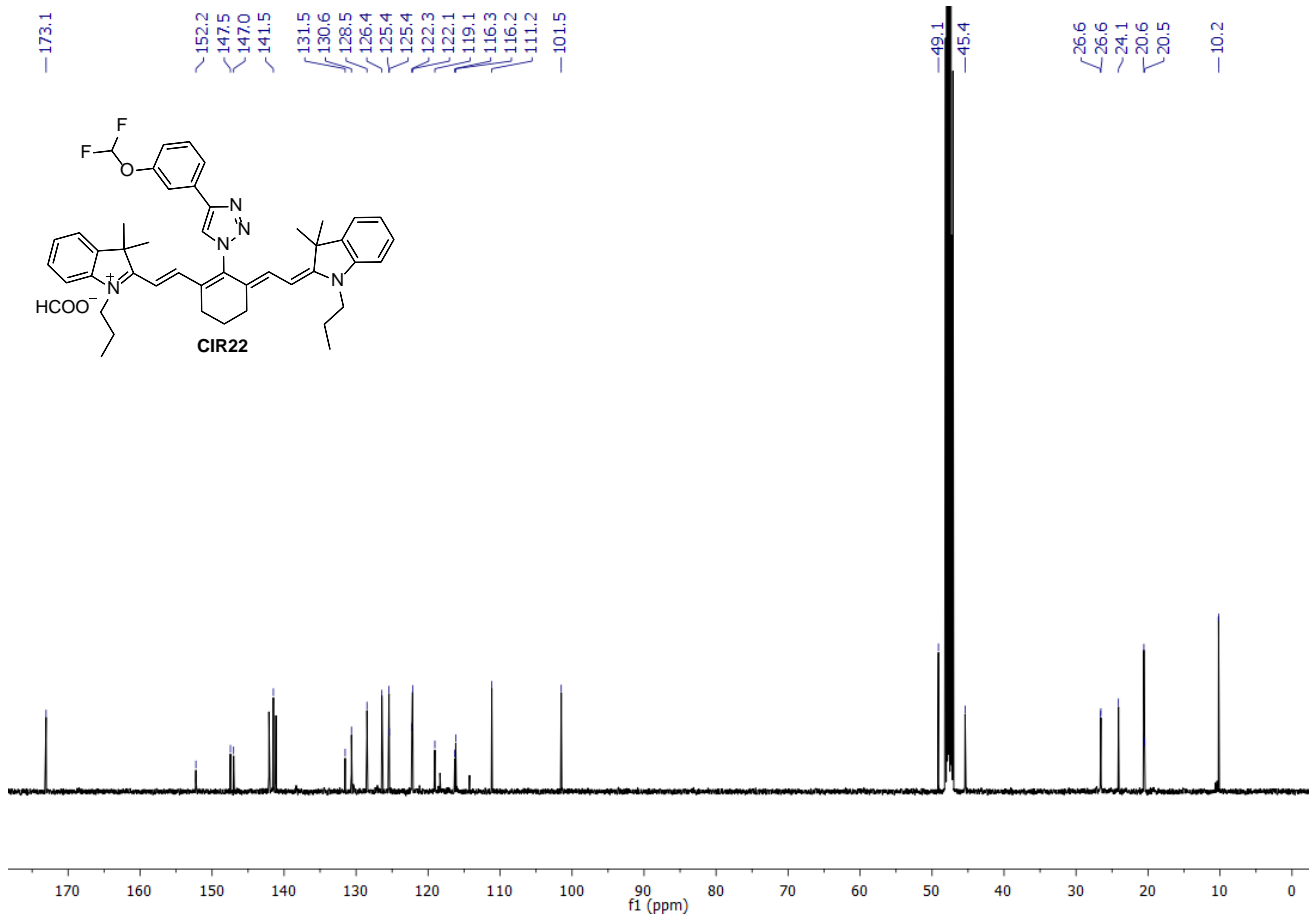
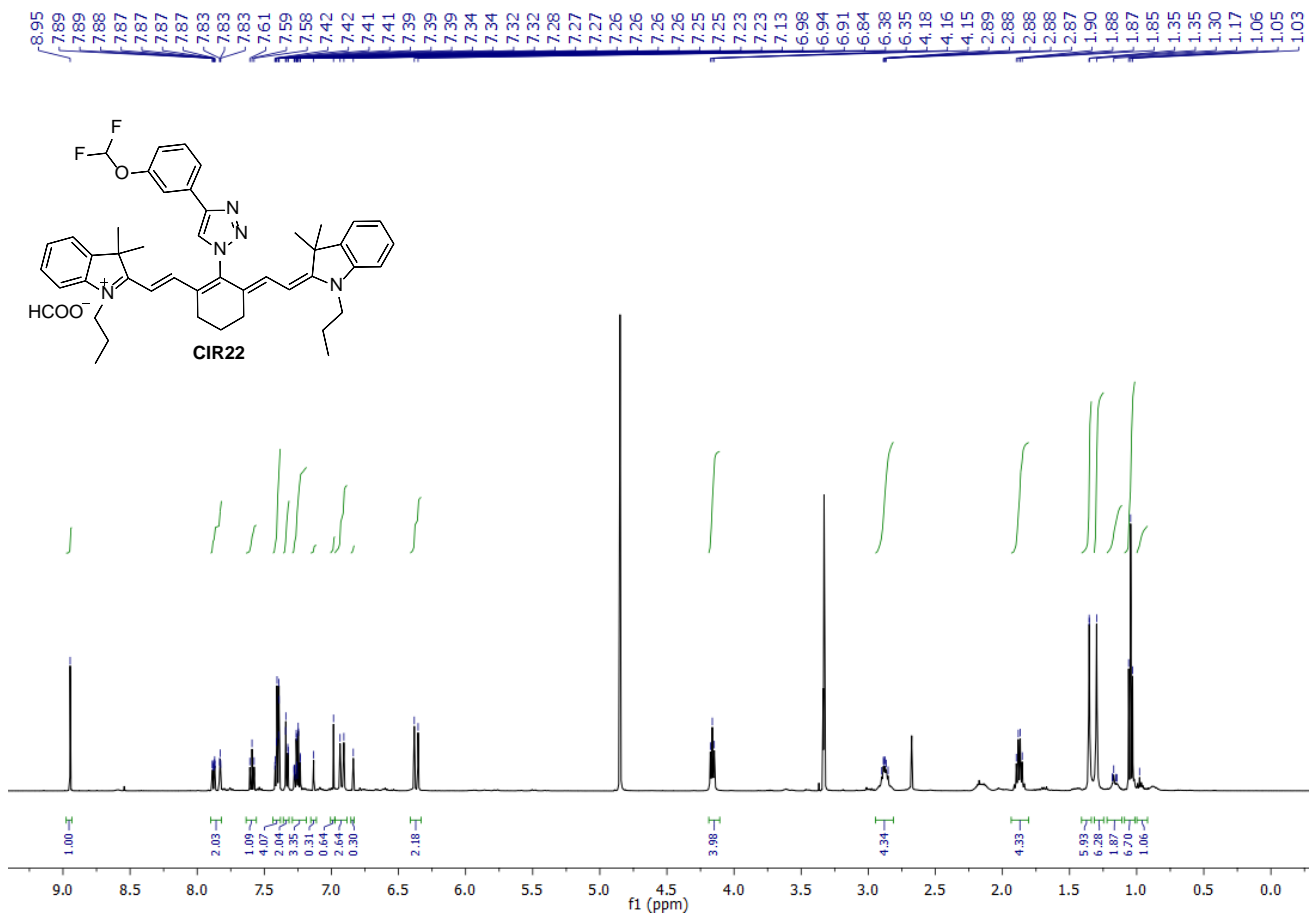


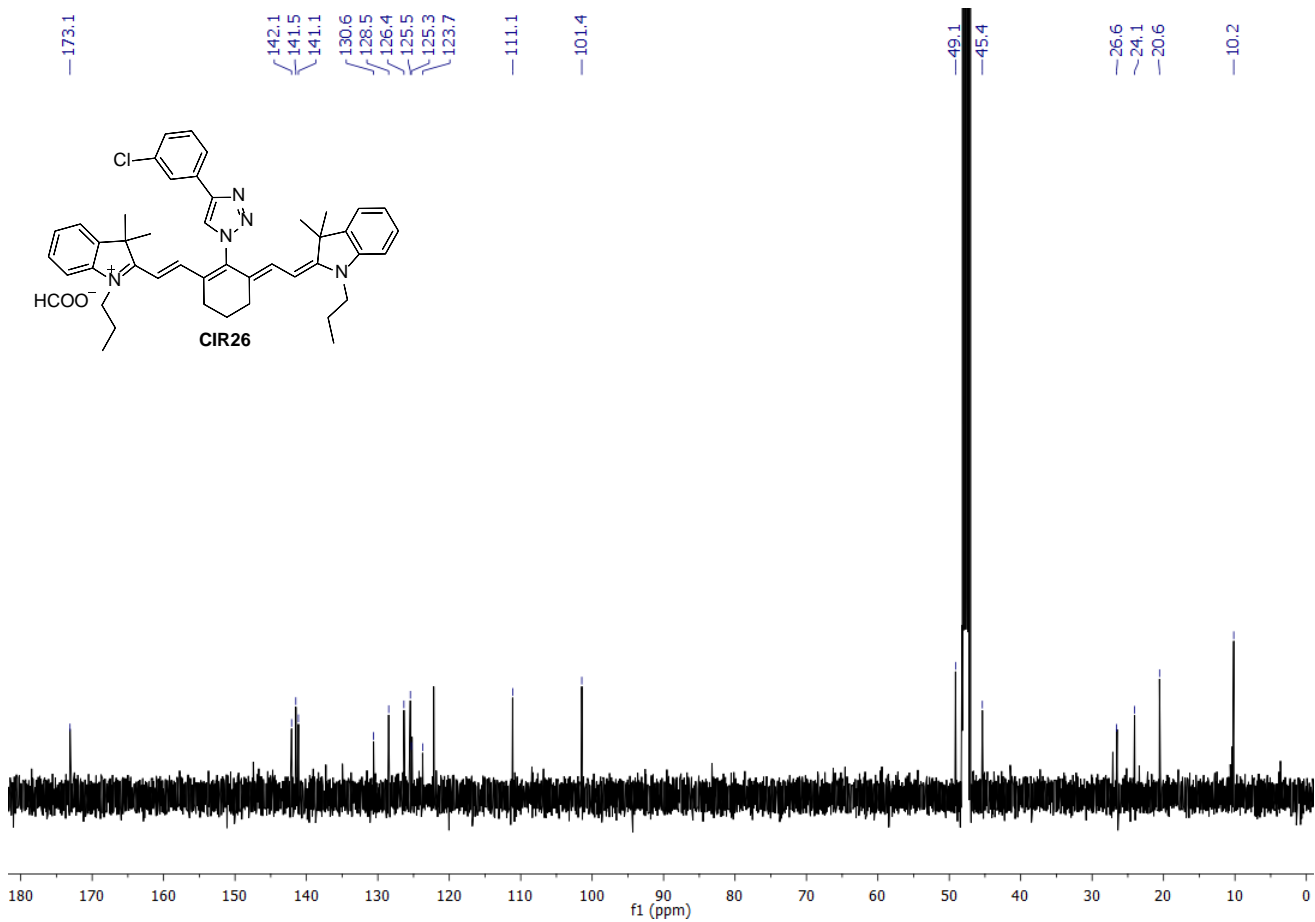
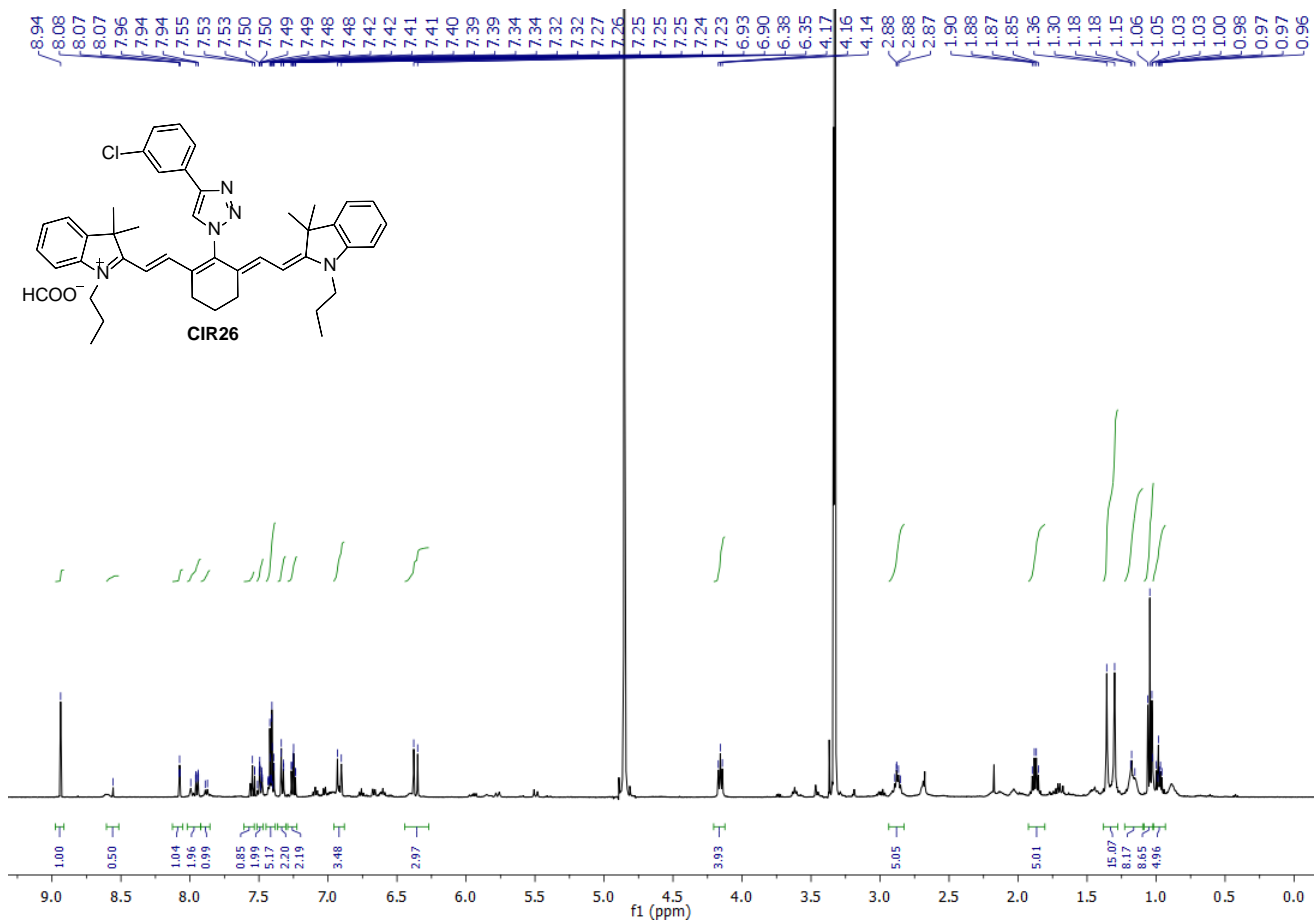


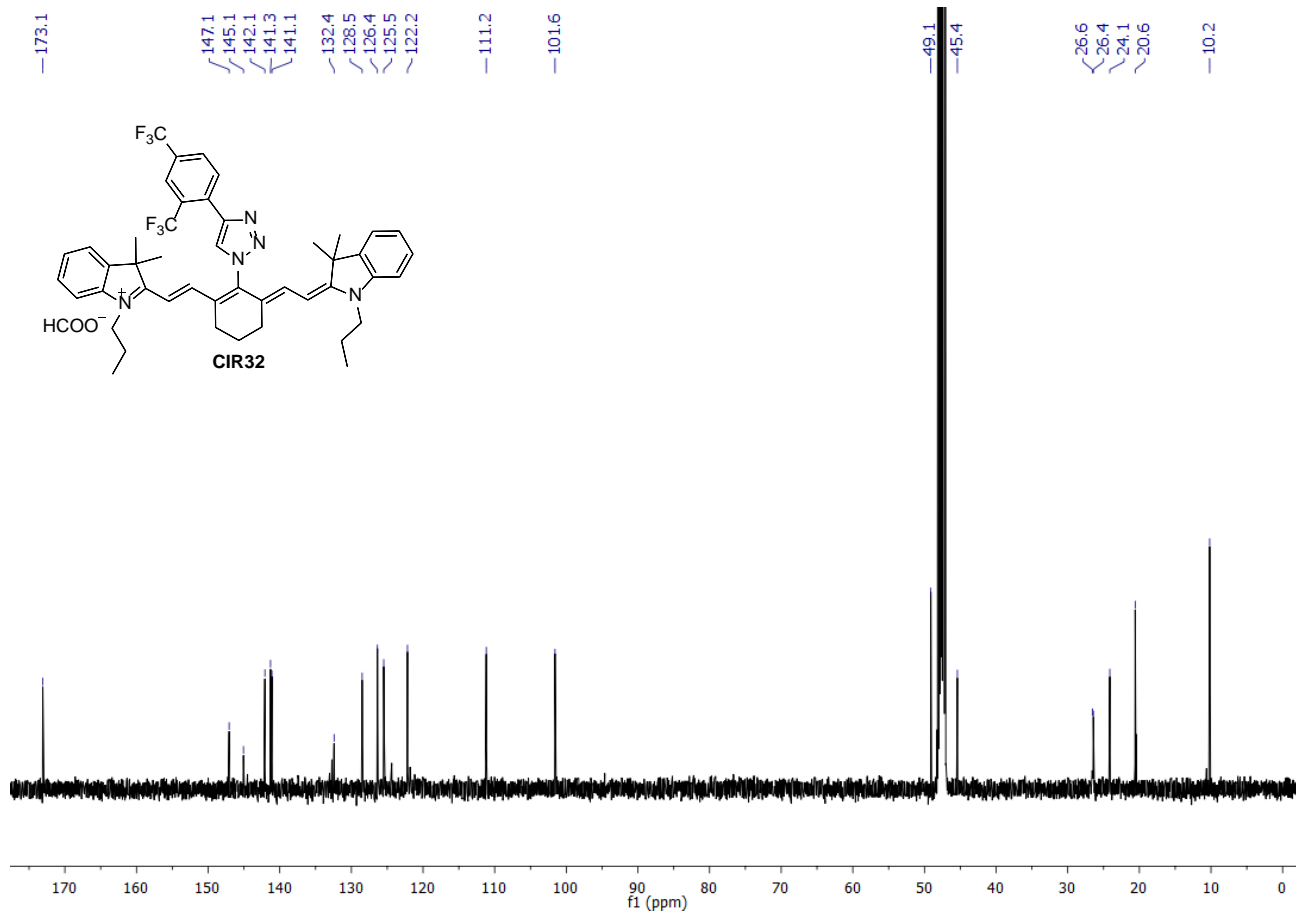
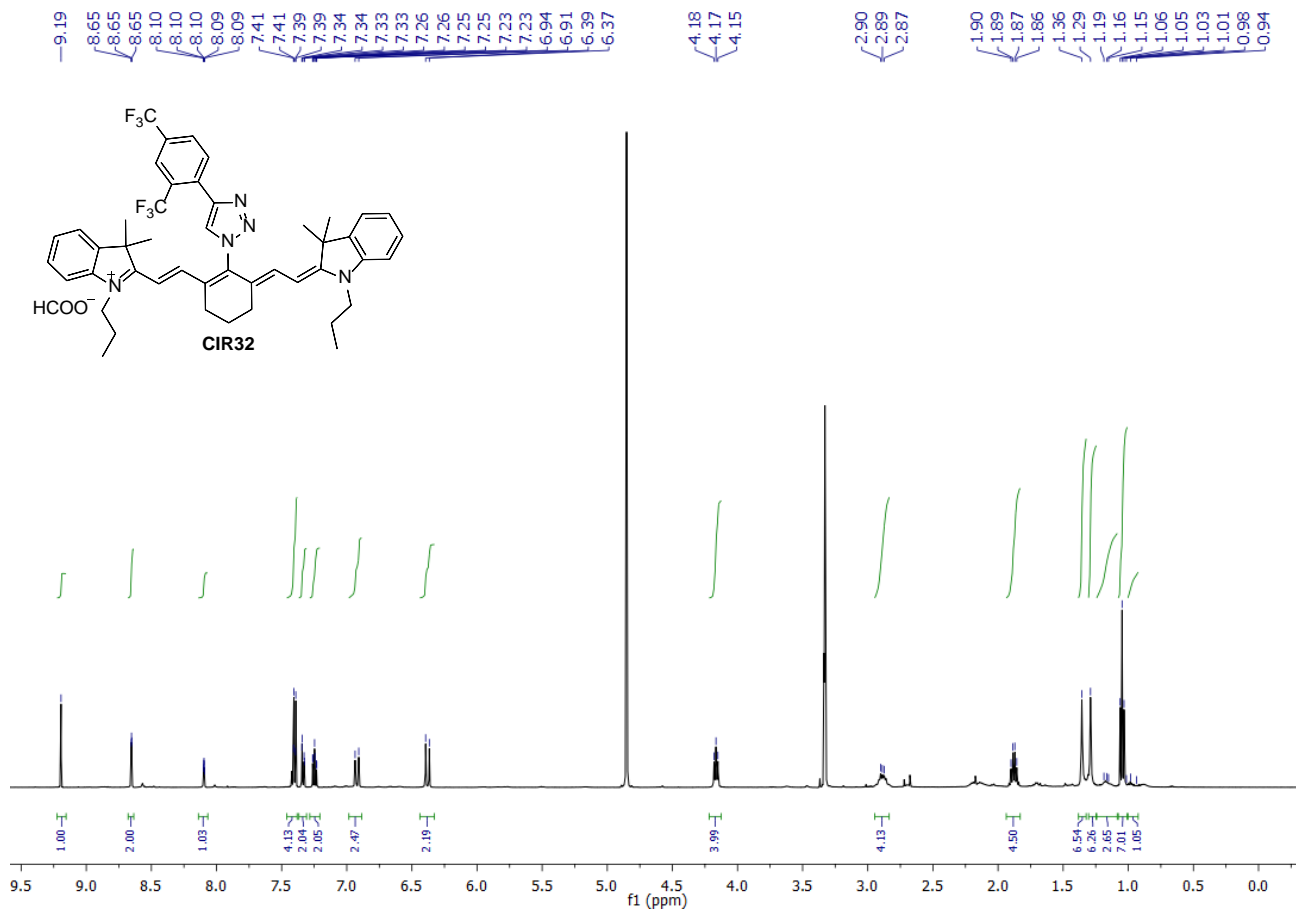


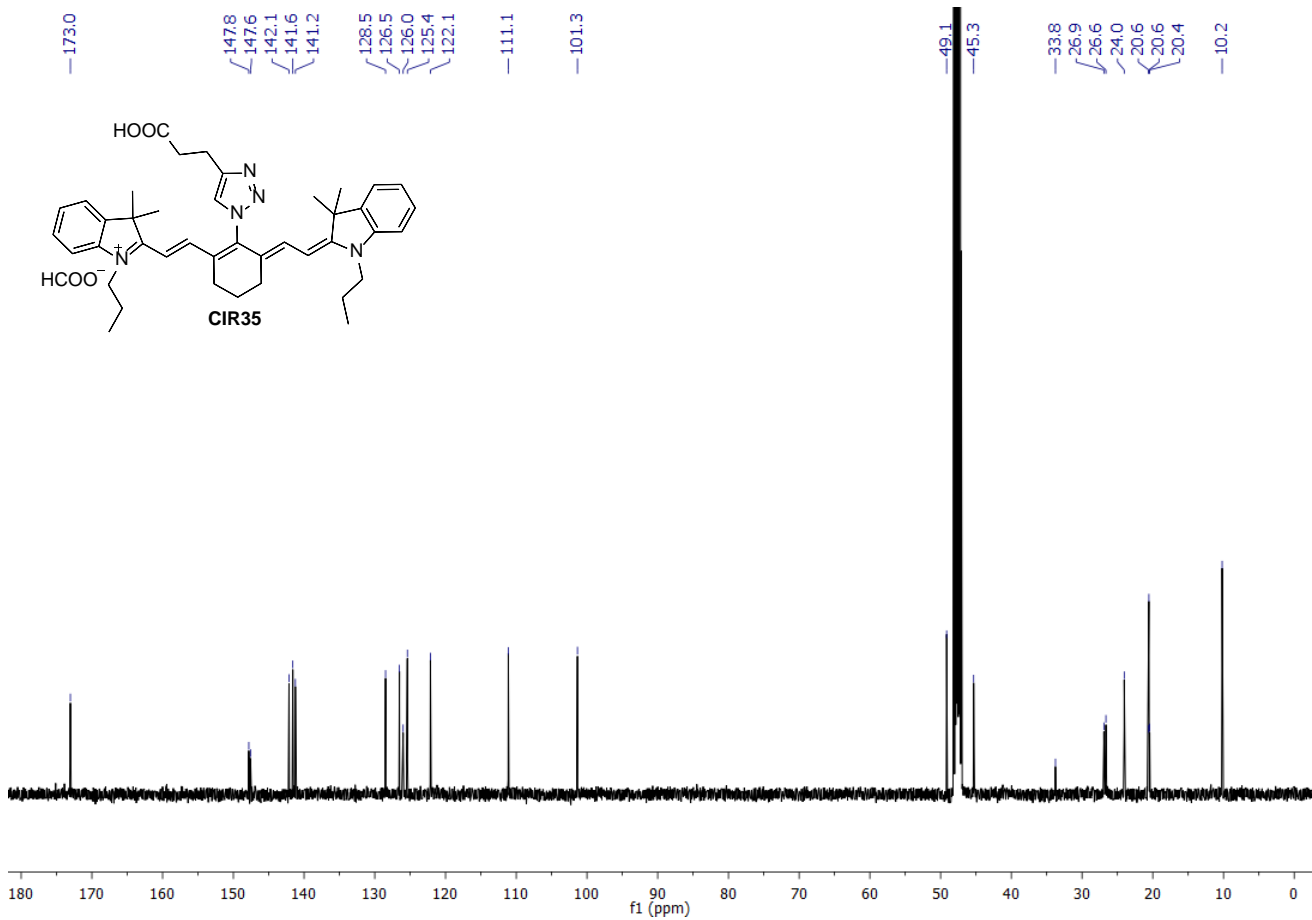
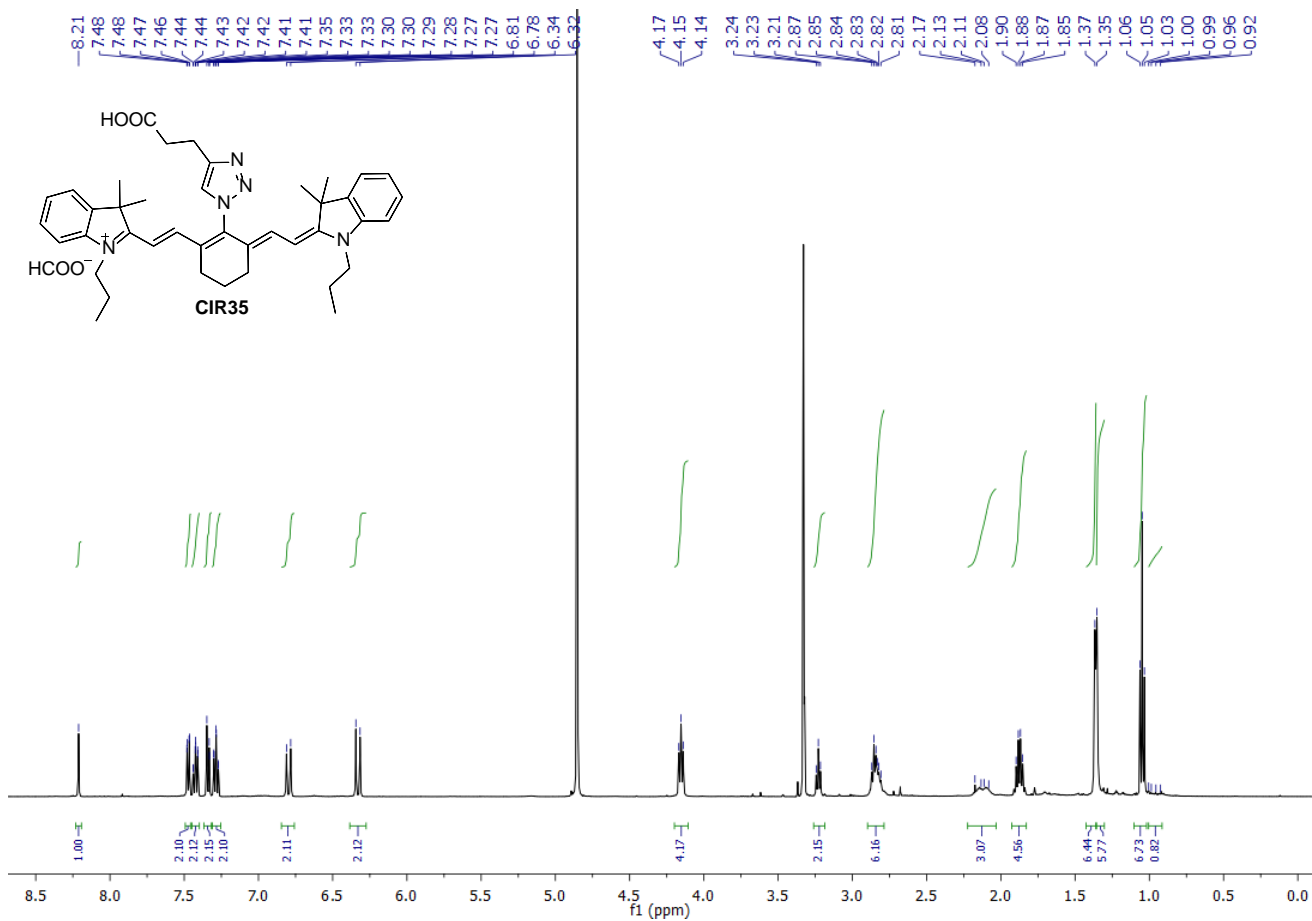


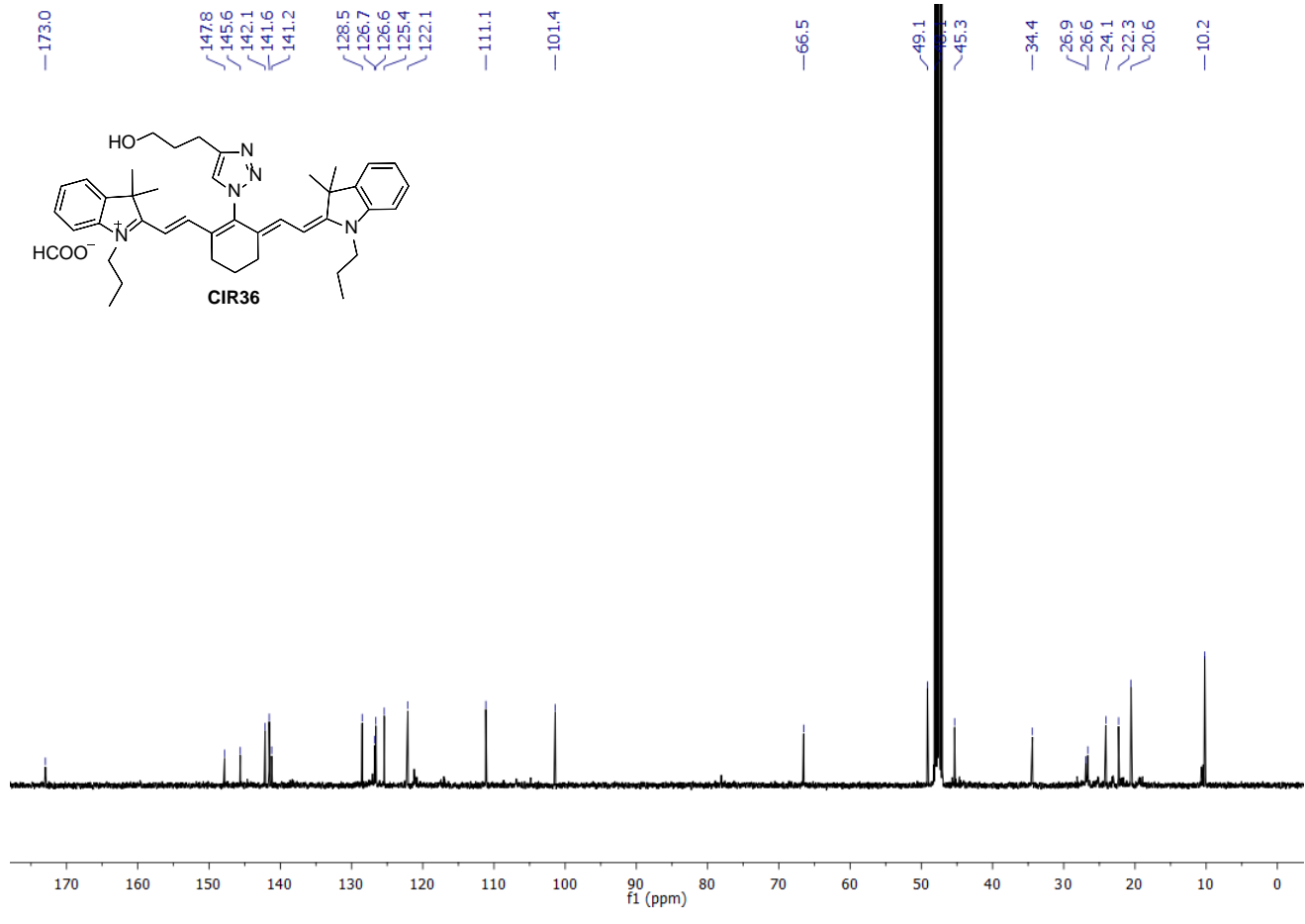
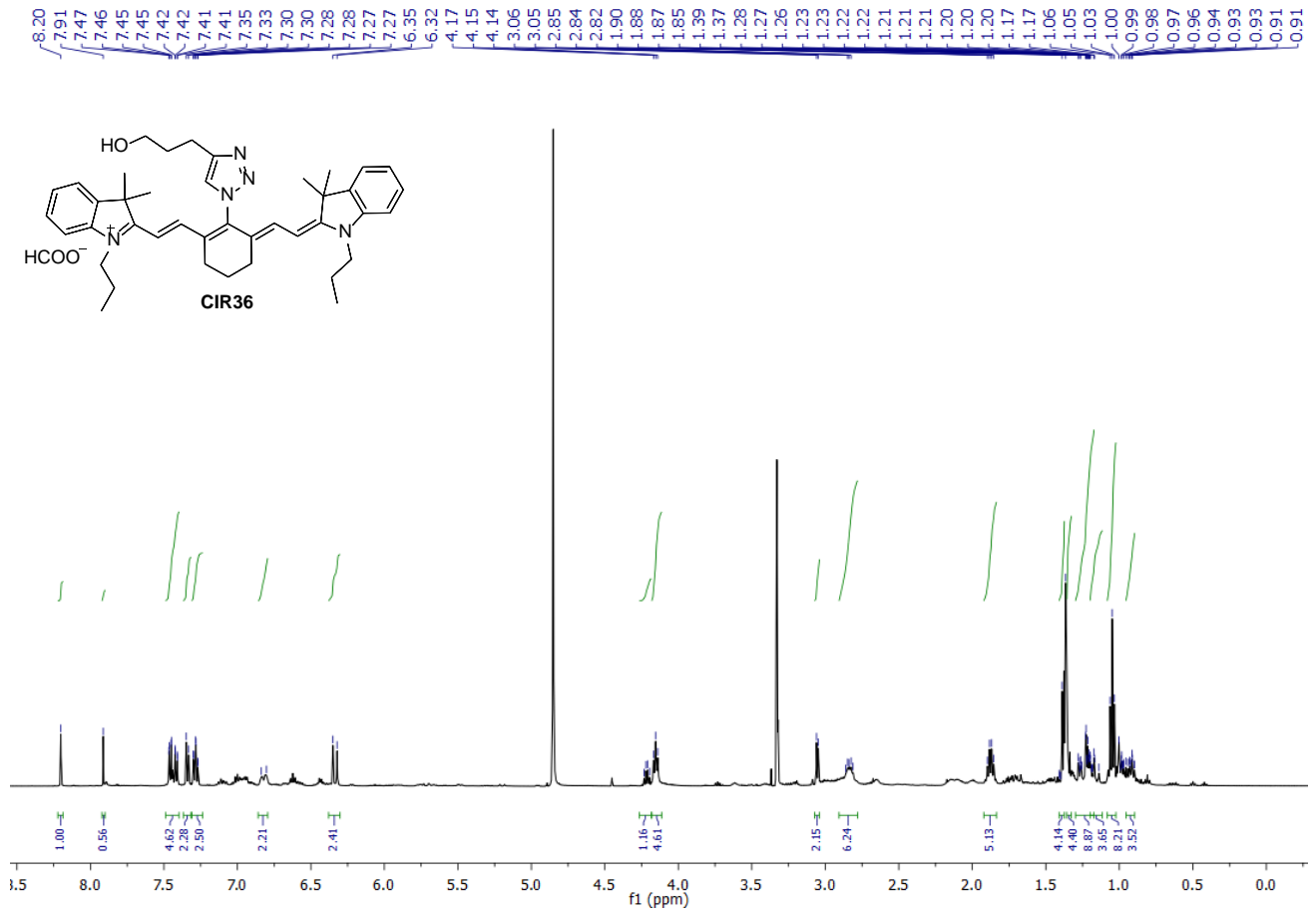


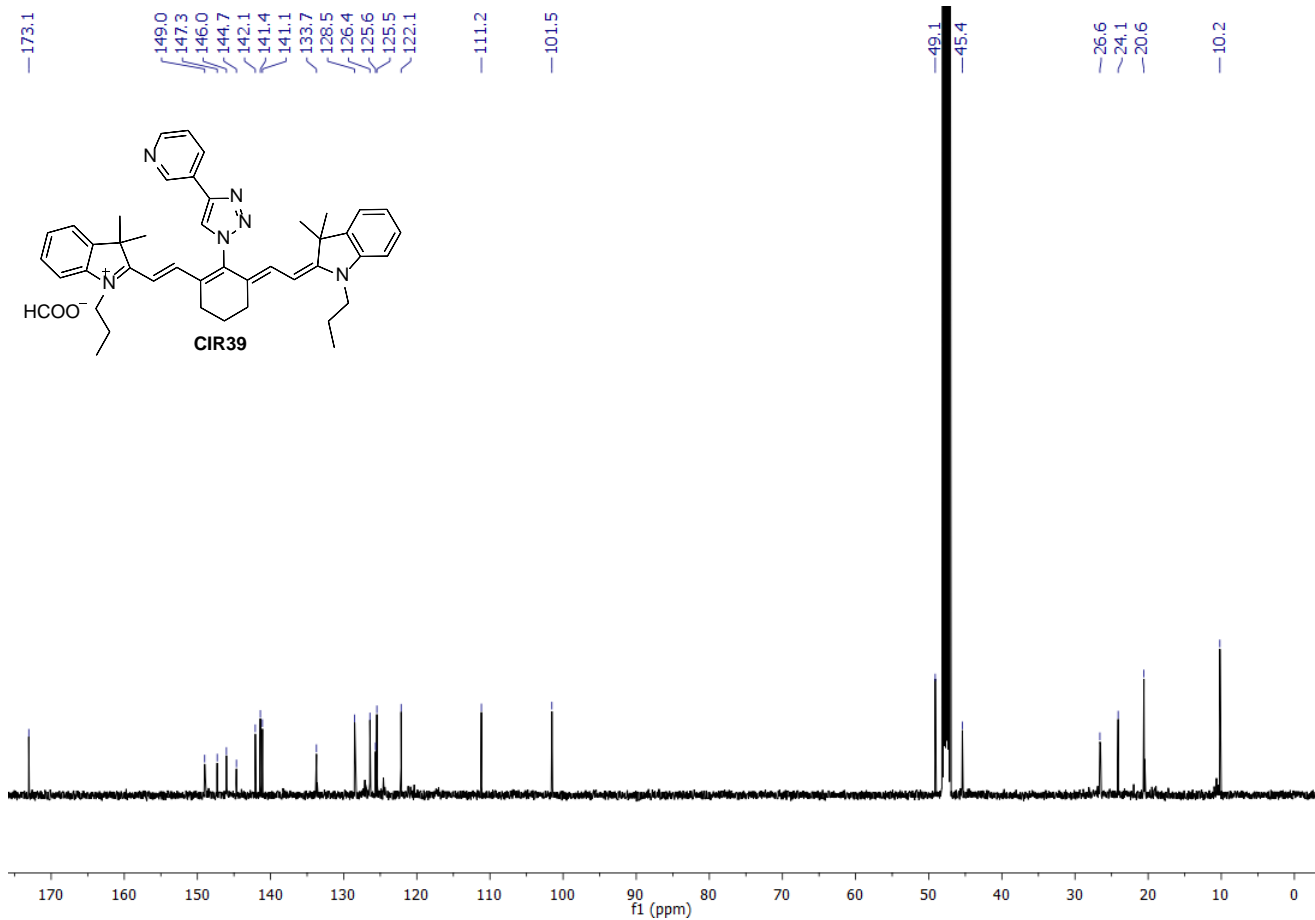
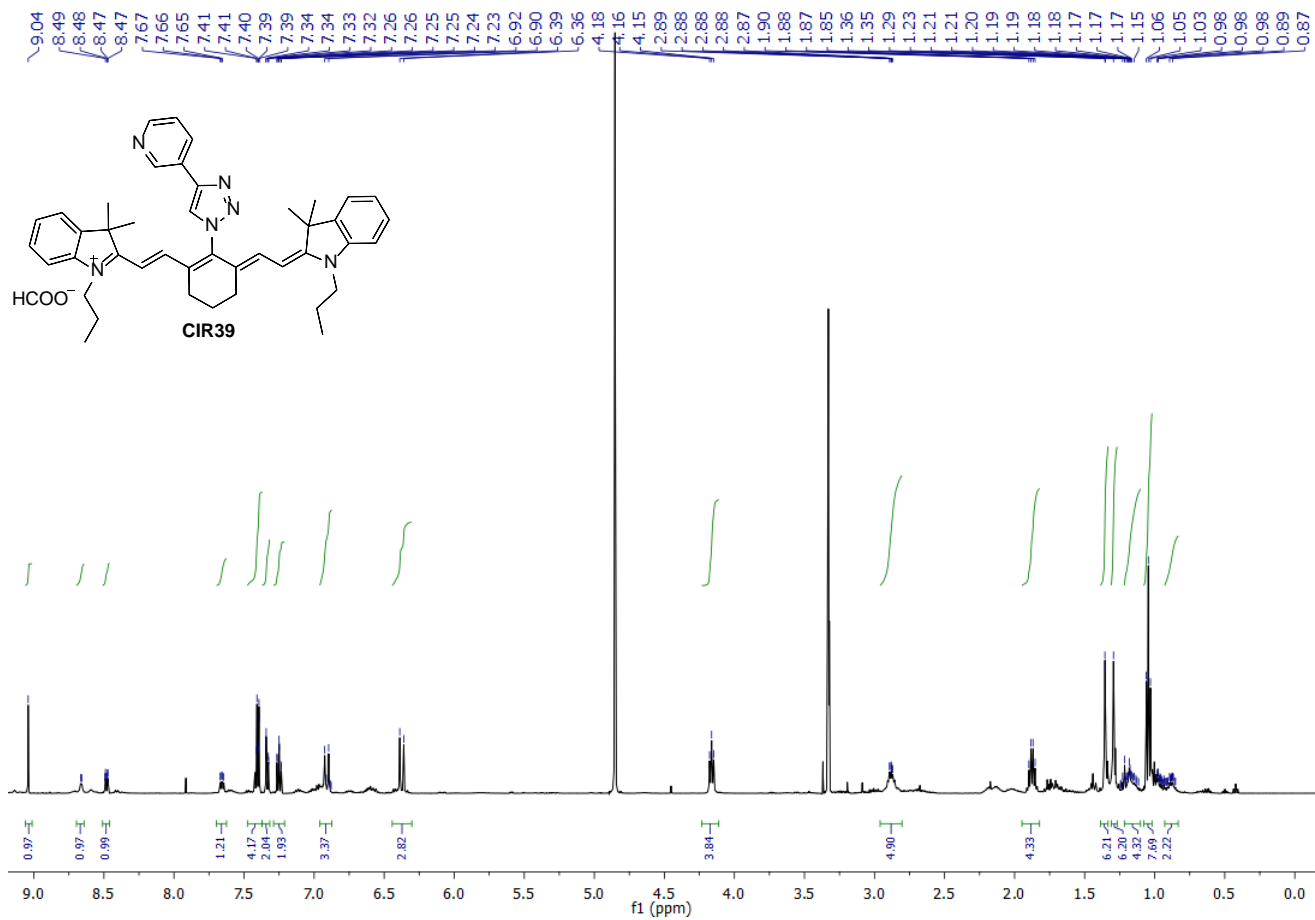












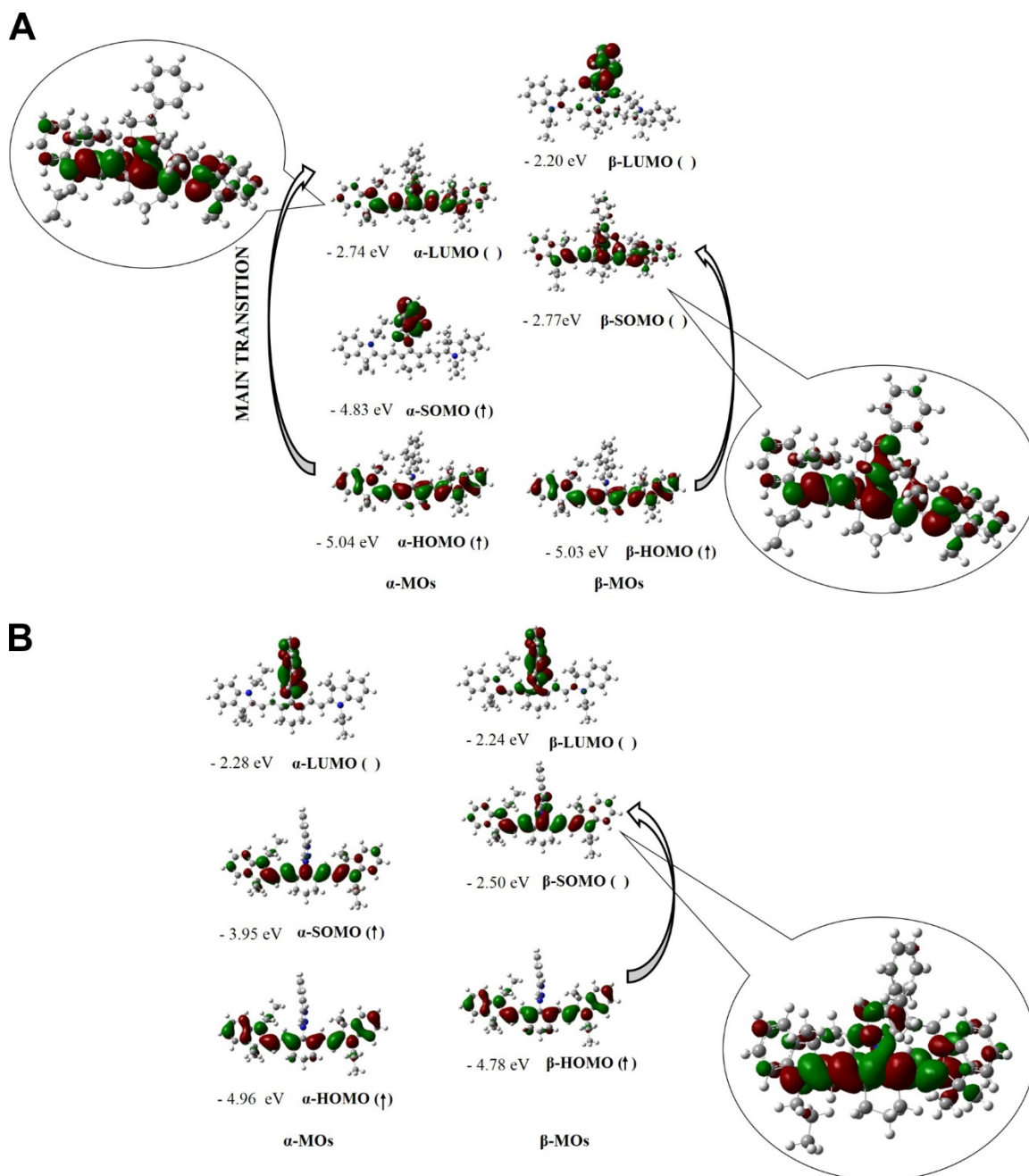


Fig. S1. Shape and energy of frontier orbitals for compound **1** (A) and compound **2** (B), calculated at the B3LYP/6-31G* level using EtOH as the solvent.

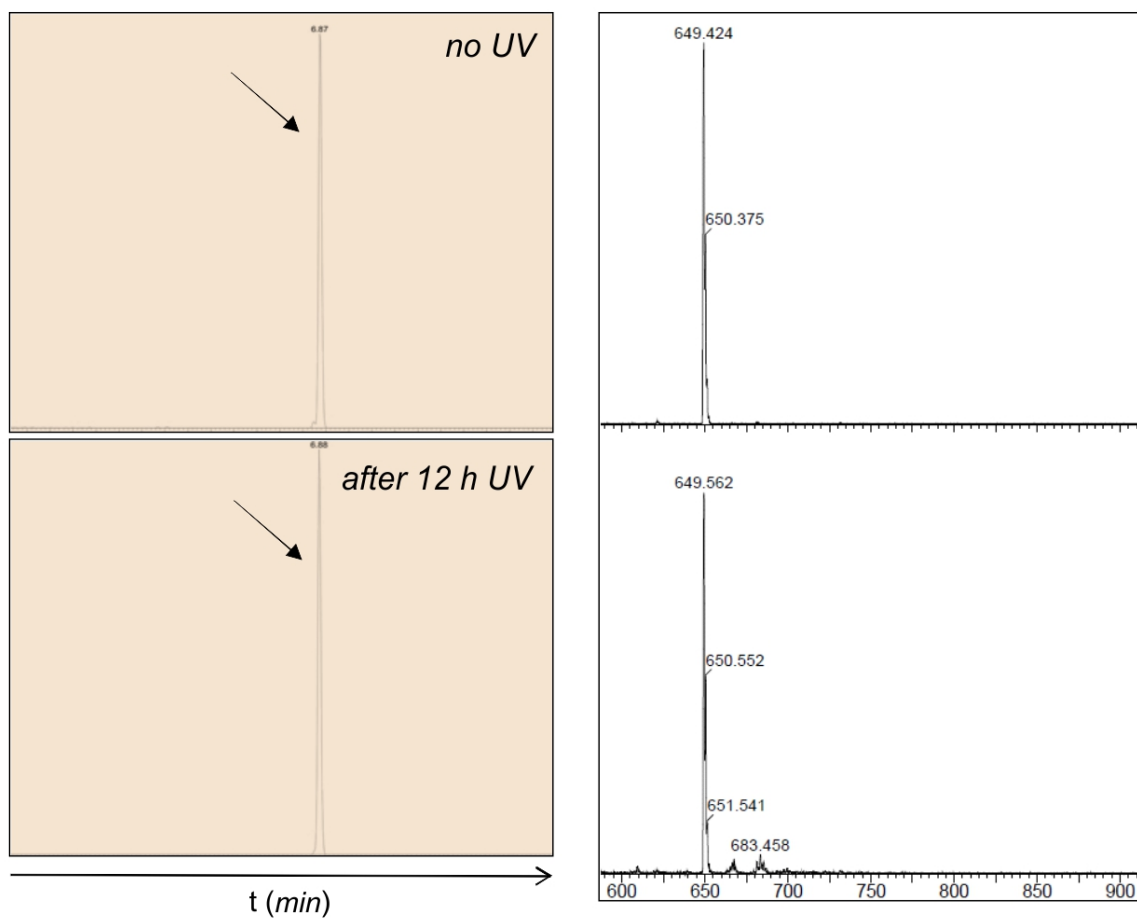


Fig. S2. HPLC-MS analysis (*left*: UV detection, *right*: MS detection) of **CIR38** before and after 12 h irradiation. Arrows pointing at intact **CIR38** (M^+ _{calc.}: 649.4).

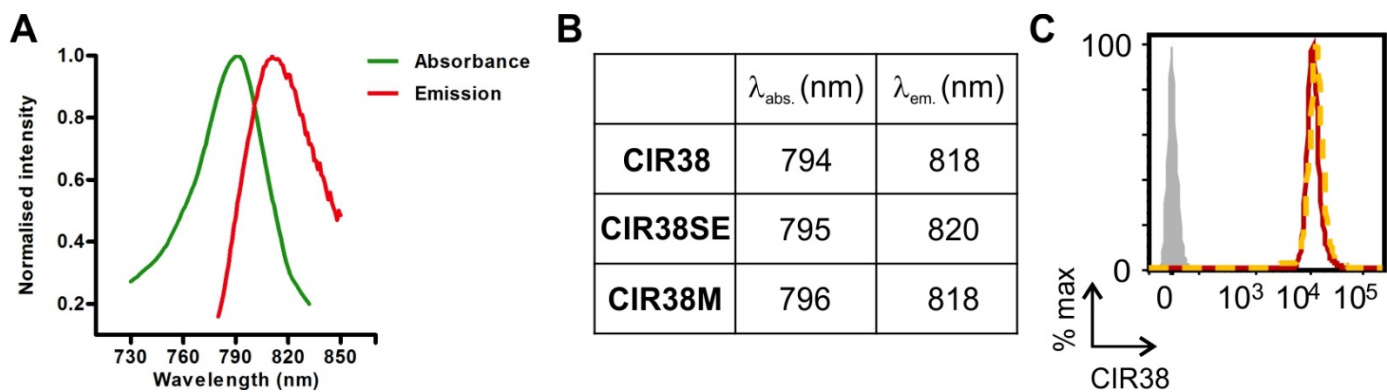


Fig. S3. A) Absorbance and fluorescence spectra of **CIR38M** in PBS. B) Summary table for the spectral characterisation data of **CIR38** derivatives in EtOH. C) Flow cytometric analysis and NIR fluorescence emission of CD4+ T cells after labelling with **CIR38SE** (dashed orange) or **CIR38M** (solid red) under the same experimental conditions (10 μM) in comparison to unlabelled cells (grey shaded area).

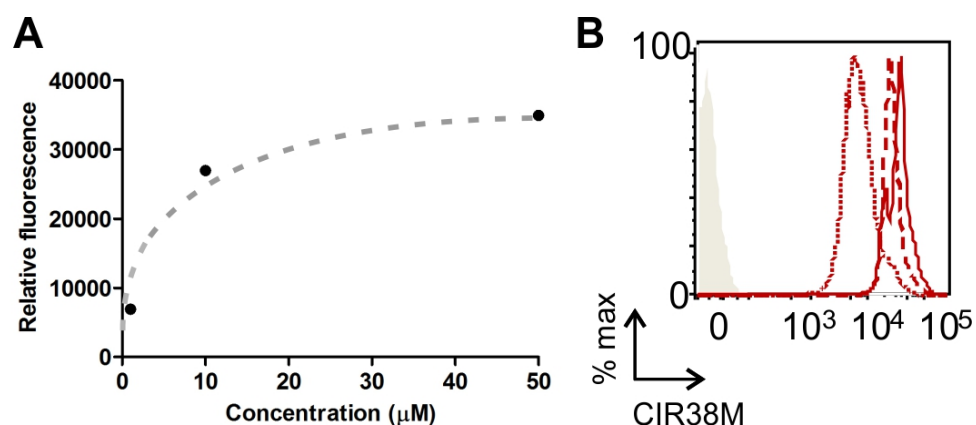


Fig. S4. A) Fluorescence saturation curve for **CIR38M** upon labelling CD4+ T cells. B) Flow cytometric analysis and NIR fluorescence emission of CD4+ T cells after labelling with **CIR38M** at different concentrations (1 μM : dotted line, 10 μM : dashed line, 50 μM : solid line) in comparison to unlabelled cells (grey shaded area).

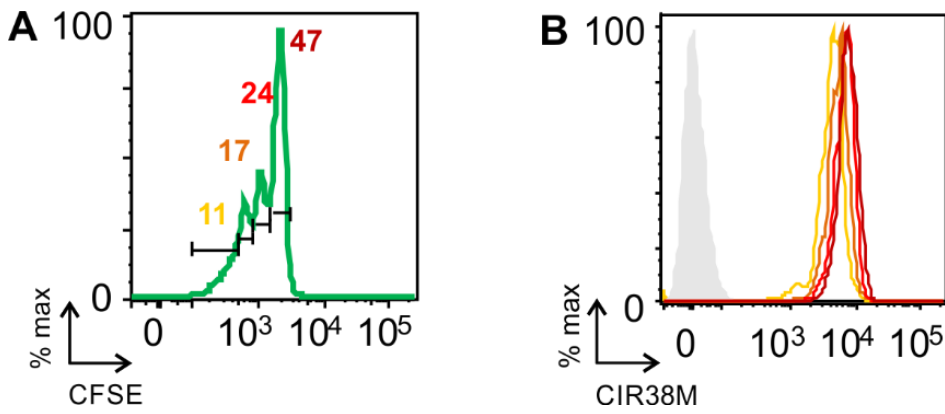


Fig. S5. A) Murine CD4+ T cells were simultaneously labelled with **CIR38M** and **CFSE** before culturing on anti-CD3 and anti-CD28 coated plates. After 3 days of *in vitro* culture, cells were analyzed by flow cytometry and categorized by their number of cell divisions as determined by **CFSE** dilution. **CFSE** fluorescence intensity was used to split the cells into four populations: undivided (accounting for 47% of the total, dark red), cells undergoing one round of proliferation (24% total, light red), two rounds of proliferation (17% total, orange) and three or more rounds of proliferation (11% total, yellow). B) **CIR38M** fluorescence emission on the four cell populations defined in A.

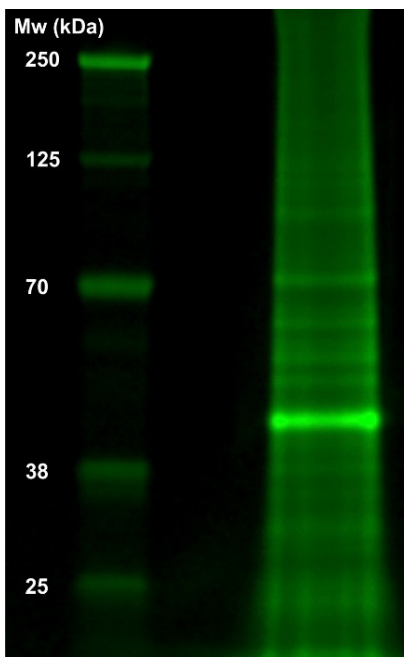


Fig. S6. SDS-PAGE analysis of lysates from CD4+ T cells upon labelling with **CIR38M** and visualisation under an Odyssey® CLx imaging system ($\lambda_{exc.} \sim 800$ nm). Protein ladder: Chameleon 800 (LI-COR).

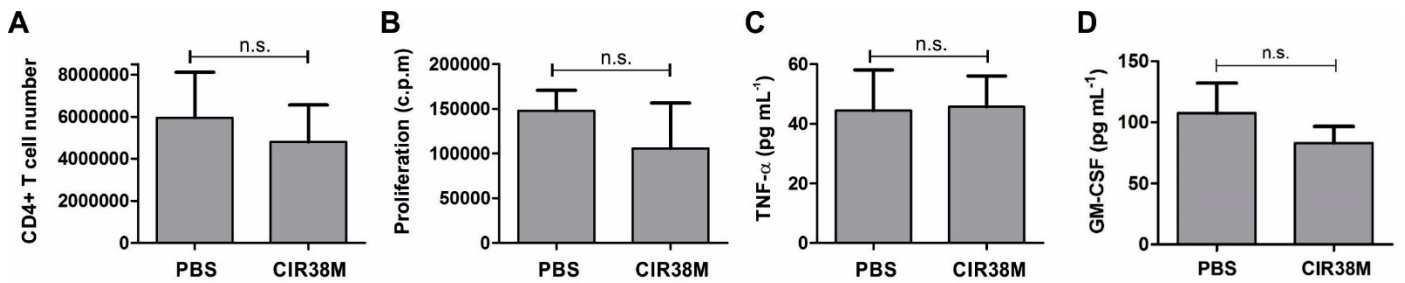


Fig. S7. A) Equal numbers of CD4⁺ T cells were labelled with **CIR38M** or treated with PBS, incubated in culture media overnight at 37 °C, and viable cells were counted 24 h later. Values are represented as means \pm s.d. (n=3). B) CD4⁺ T cells were labelled with **CIR38M** or treated with PBS and subsequently cultured on anti-CD3 and anti-CD28 coated plates. After 48 h, cell proliferation was assessed by the addition of [³H]-thymidine for the last 18 h of culture. Values are represented as means \pm s.d. (n=3). C) CD4⁺ T cells were labelled with **CIR38M** or treated with PBS and subsequently cultured on anti-CD3 and anti-CD28 coated plates. TNF- α concentrations in the supernatant were determined by ELISA 72 h later. Values are represented as means \pm s.d. (n=3); $p > 0.05$ for n.s. D) ELISA determination of cytokine production by **CIR38M**-labelled and unlabelled CD4⁺ T cells. Values are represented as means \pm s.d. (n=6 per group). $p > 0.05$ for n.s.

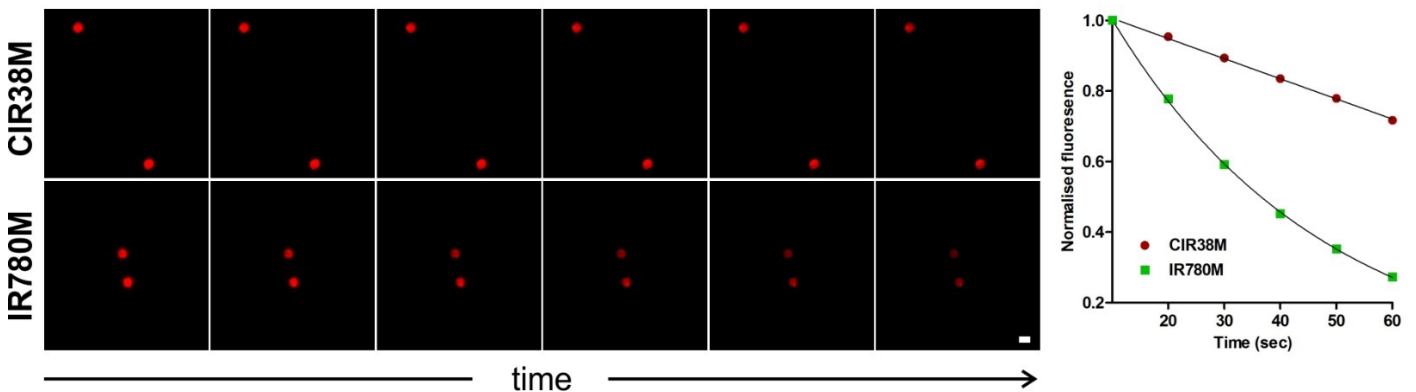


Fig S8. Time-lapse comparative NIR cell imaging of **CIR38M** and **IR780M**-labelled CD4⁺ T cells under fluorescence microscopy. Samples were constantly irradiated and individual images were acquired every 10 seconds for a total of 1 min. Scale bar: 5 μ m. Normalised fluorescence intensity values for both sets of images were fitted to one phase exponential decay regressions (left plot).

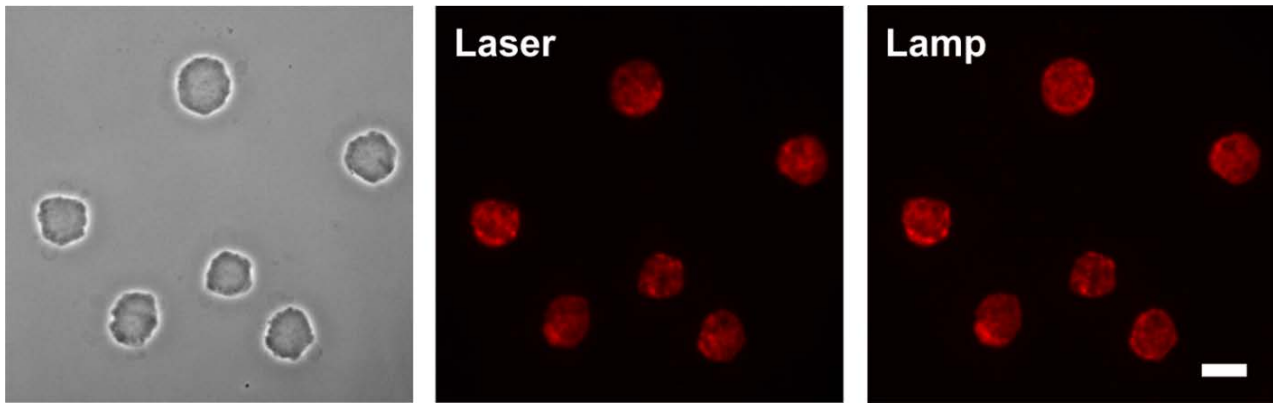


Fig. S9. Comparative fluorescence cell imaging of **CIR38M**-labelled CD4+ T cells under a fluorescence microscope equipped with Ti-sapphire laser and mercury lamp excitation sources.

Scale bar: 5 μm .

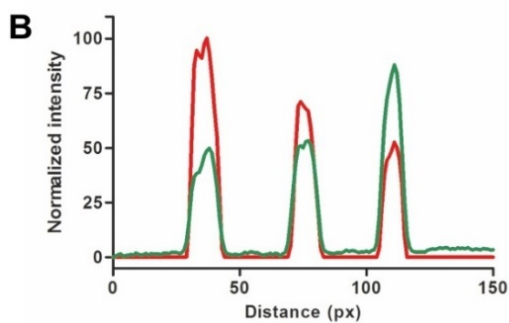
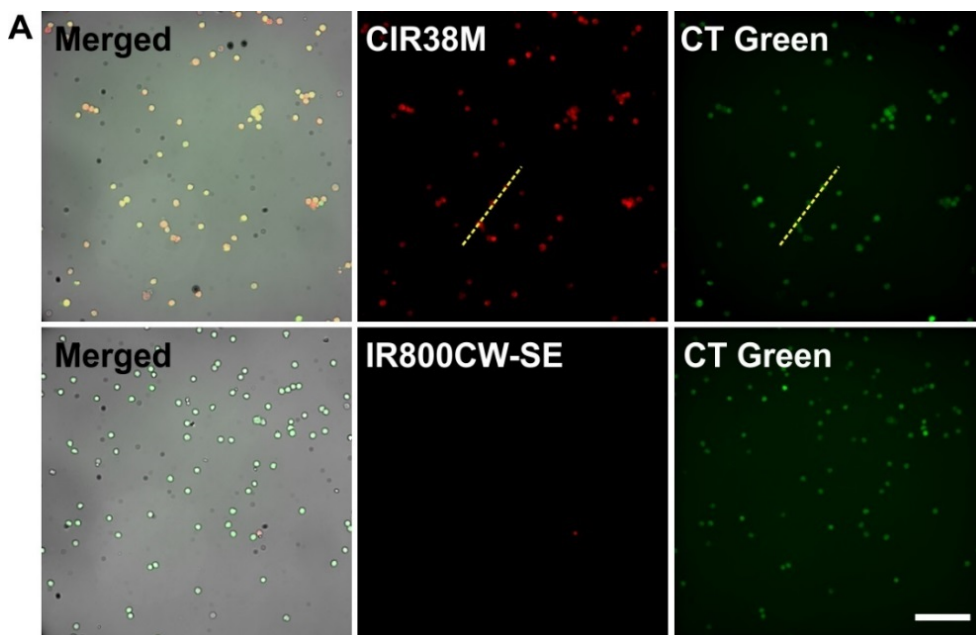


Fig. S10. A) Low-magnification fluorescence microscopy images of CD4+ T cells upon staining with CellTracker Green (green) and **CIR38M** or **IR800CW-SE** (red). Scale bar: 50 μm . B) Plot profile analysis of the dashed yellow line in the top panel in (A), which correlates the intracellular staining of **CIR38M** (red) to CellTracker Green (green).

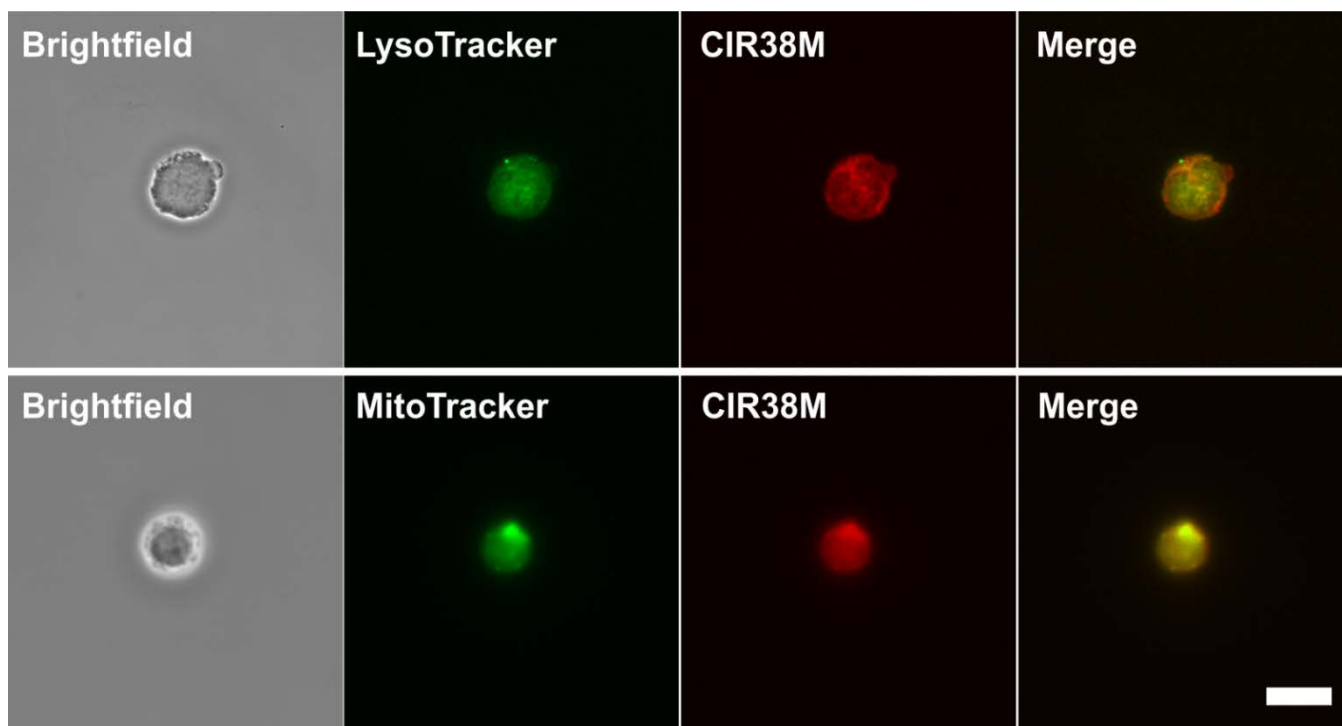


Fig. S11. High-magnification fluorescence microscopy images of CD4+ T cells upon co-staining with LysoTracker Red DND-99 (100 nM, green), MitoTracker Red CMXRos (500 nM, green) and **CIR38M** (10 μ M, red). Scale bar: 5 μ m.

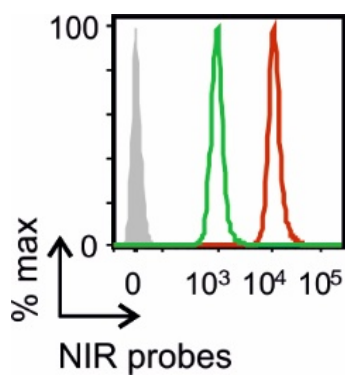


Fig. S12. Flow cytometric analysis CD4+ T cells upon labelling with 10 μ M **CIR38M** (red line), 10 μ M **IR800CW-SE** (green line), or left unstained (grey shaded area).

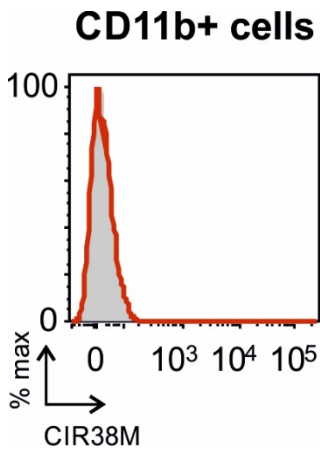


Fig. S13. Histogram depicting lack of fluorescence in host CD11b+ myeloid cells retrieved from the iLNs from mice injected with **CIR38M**-labelled CD4+ T cells (red line) and with unlabelled CD4+ T cells (grey shaded area) on day 7.

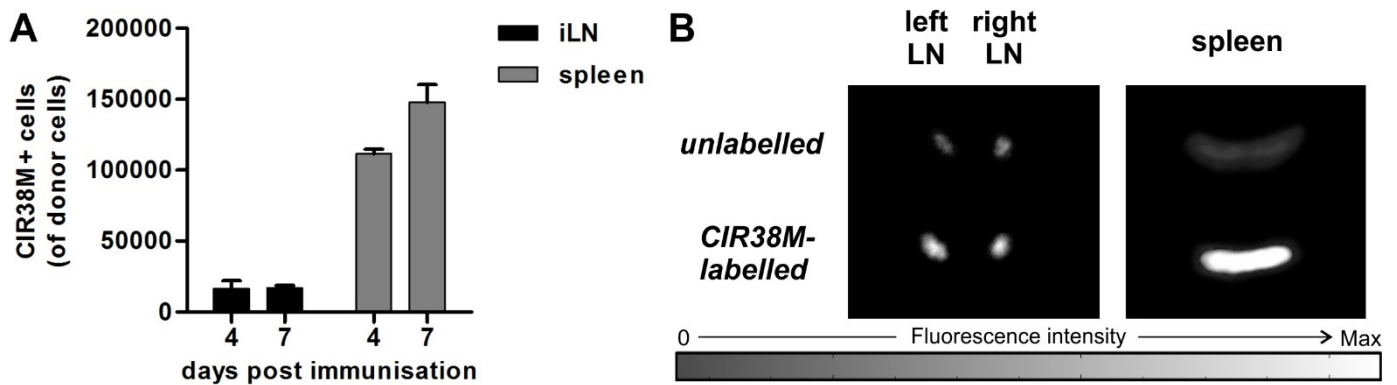


Fig. S14. Mice were injected i.v. with **CIR38M**-labelled pOVA-reactive CD45.1+ CD4+ OT-II T cells and immunised by injection of 50 μ L of 10 μ g mL⁻¹ pOVA in CFA. Mice were sacrificed and inguinal lymph nodes (iLN) and spleens harvested on days 4 or 7. A) Total numbers of **CIR38M**-positive donor cells were determined by flow cytometry. Values are represented as means \pm s.e.m (n=3 per group). B) *Ex vivo* tissue fluorescence images ($\lambda_{exc.}$ ~ 760 nm; $\lambda_{em.}$ ~ 800-900 nm) of lymph nodes and spleen tissue from mice that had been injected the same amount of **CIR38M**-labelled or unlabelled T cells for 7 days. Max: 5×10^7 photons s⁻¹.

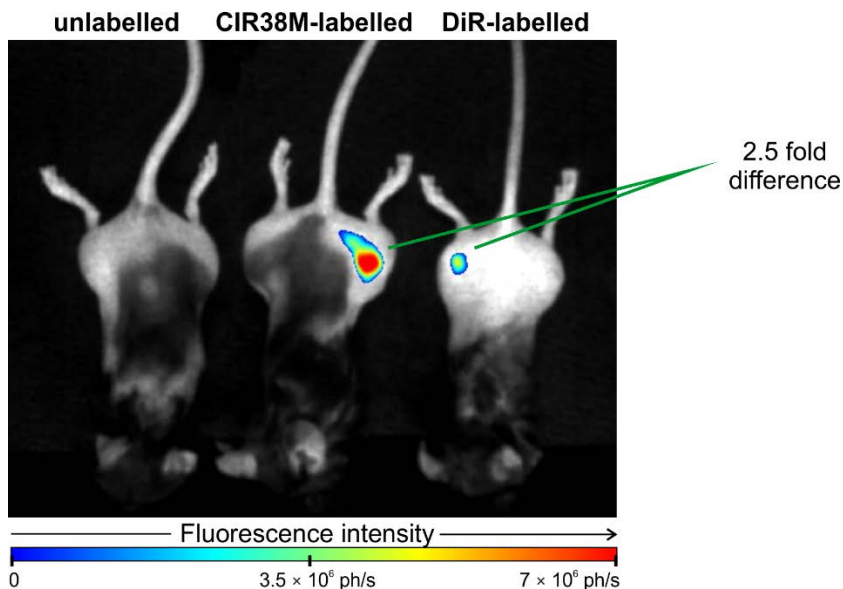


Fig. S15. Whole-body fluorescence images ($\lambda_{exc.} \sim 760$ nm; $\lambda_{em.} \sim 800-900$ nm) of B10.PLxC57BL/6 mice (representative image from 3 mice pairs) 2 days after the tail vein i.v. injection of **DiR**-labelled (right), **CIR38M**-labelled (center) or unlabelled CD4+ Tg4 T cells (left). Cell transfer was followed by subcutaneous immunisation with 10 μ g of MBP Ac1-9(4Tyr) peptide emulsified in CFA containing 50 μ g of heat-killed *Mycobacterium tuberculosis* H37Ra at a total final volume of 100 μ L injected subcutaneously into the hind legs.

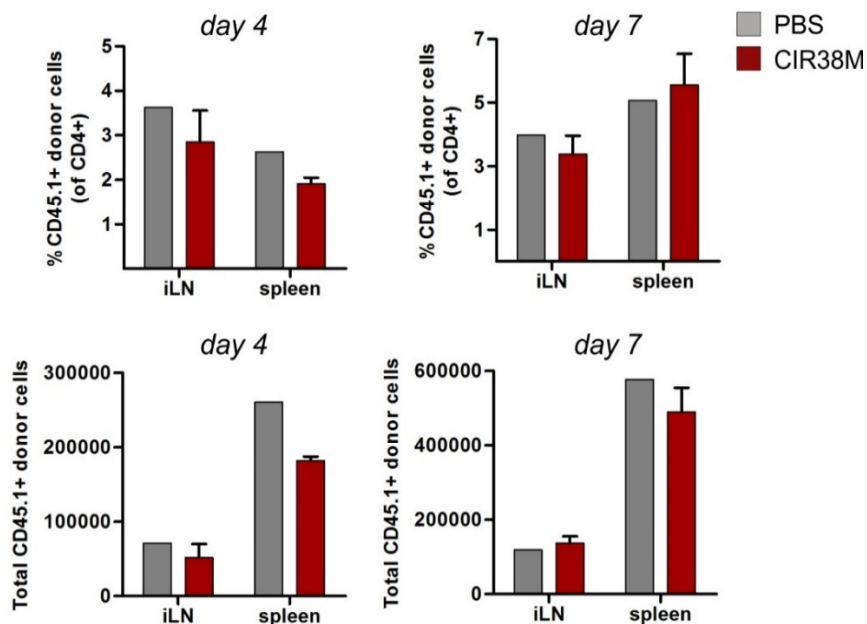


Fig. S16. Proportion and total numbers of CD45.1+ donor cells retrieved from iLNs and spleen on days 4 or 7. Values are represented as means \pm s.e.m (n=3 for the **CIR38M**-labelled group).

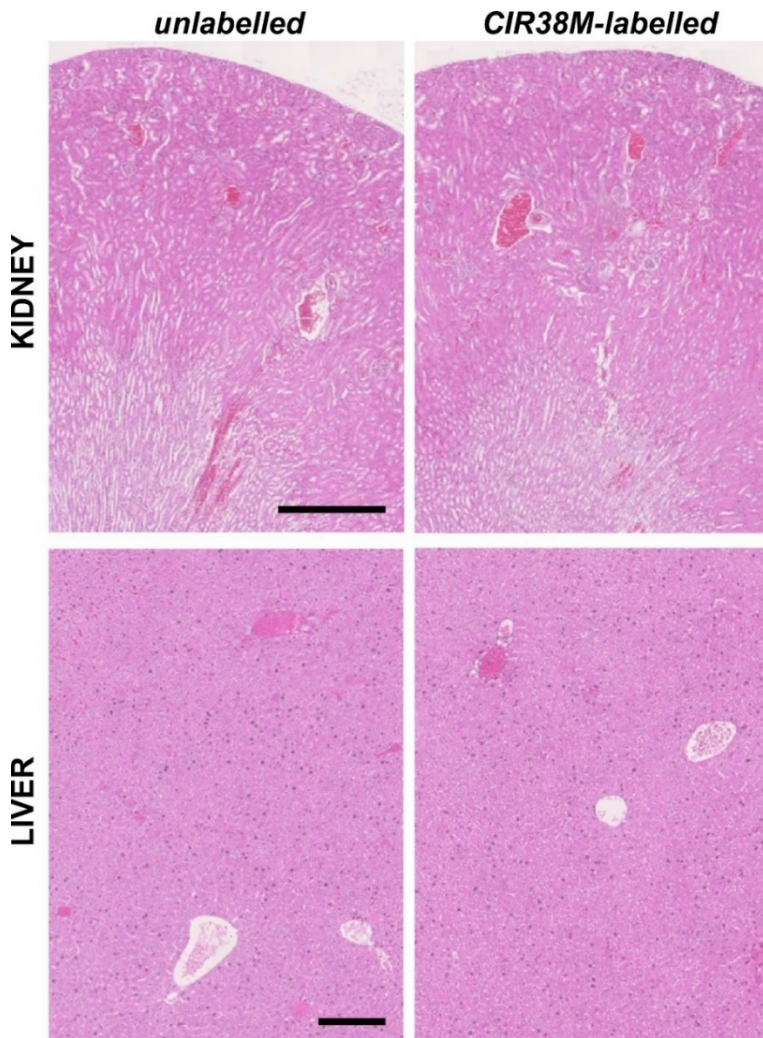


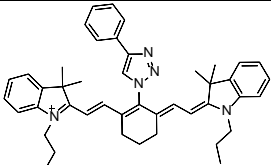
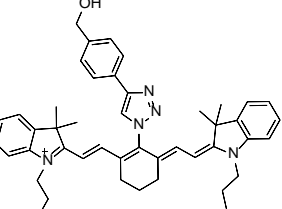
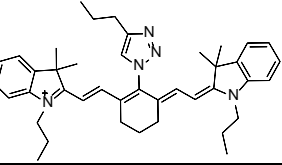
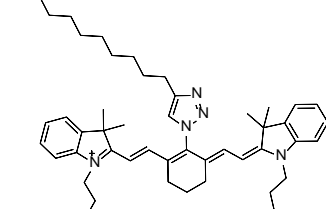
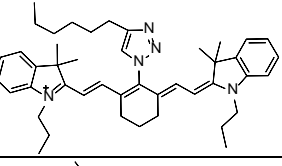
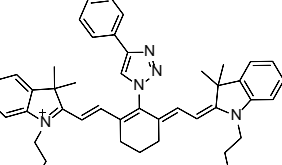
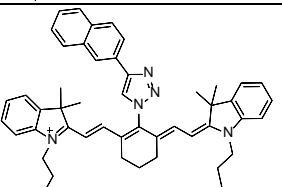
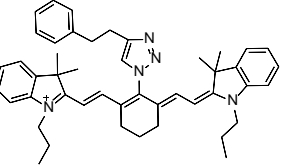
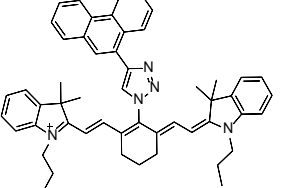
Fig. S17. Histological analysis of kidney (*top panels*) and liver (*bottom panels*) tissues from mice that had been injected with unlabelled or **CIR38M**-labelled CD4⁺ T cells and immunised with pOVA and CFA. Tissues were harvested 2 days after cell injection, fixed in 4% neutral buffered formalin, paraffin-embedded and stained with haematoxylin and eosin (H&E). Scale bars: 500 μm (top), 200 μm (bottom).

Table S1. Electronic transitions computed for compounds **1** and **2** at the TD-B3LYP/6-31G**/B3LYP/6-31G*, TD-M06-2X/6-31G**/M06-2X/6-31G*, TD-PBE0/6-31G**/PBE0/6-31G* and TD-wB97xd/6-31G*/wB97xd/6-31G* levels of theory, in gas phase and in EtOH solution.

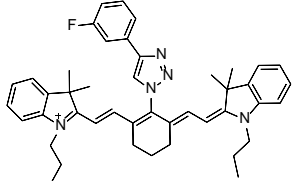
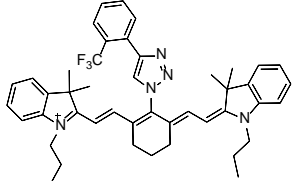
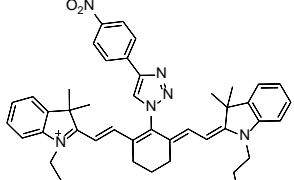
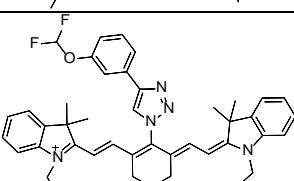
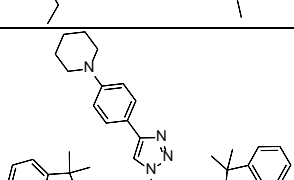
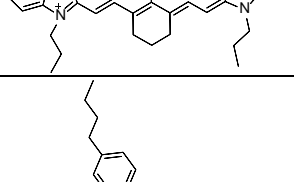
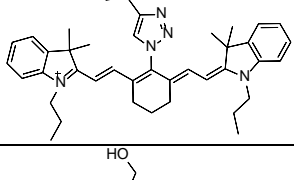
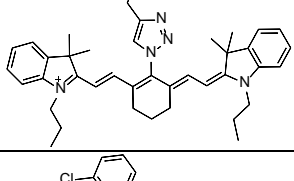
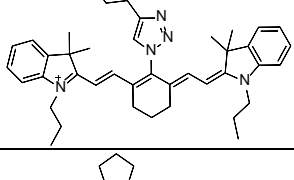
	Solvent	COMPOUND 1 (<i>N</i> -amine)				COMPOUND 2 (<i>N</i> -triazole)				
		E (eV)	λ (nm)	<i>f</i>	Main component of the transition (% contribution)	E (eV)	λ (nm)	<i>f</i>	Main component of the transition (% contribution)	
TD-B3LYP/6-31G*	EtOH	2.08	596	1.9236	α -HOMO \rightarrow α -LUMO (49.62%) β -HOMO \rightarrow β -SOMO (49.45%)	1.59	782	0.2284	α -SOMO \rightarrow α -LUMO+2 (19.08%) β -HOMO \rightarrow β -SOMO (77.29%) β -HOMO \rightarrow β -LUMO (1.61%)	
						2.35	528	2.0565	α -SOMO \rightarrow α -LUMO+2 (71.74%) β -HOMO \rightarrow β -SOMO (16.31%) β -HOMO \rightarrow β -LUMO (6.19%)	
	None	2.16	573	1.8163	α -HOMO \rightarrow α -LUMO (50.43%) β -HOMO \rightarrow β -SOMO (49.65%) α -HOMO \leftarrow α -LUMO (1.32%) β -HOMO \leftarrow β -SOMO (1.42%)	1.89	656	0.3313	α -HOMO \rightarrow α -LUMO (68.34%) β -HOMO \rightarrow β -SOMO (19.24%) β -HOMO \rightarrow β -LUMO (8.14%)	
						2.46	504	1.1710	α -SOMO \rightarrow α -LUMO+2 (46.61%) β -HOMO \rightarrow β -SOMO (6.94%) β -HOMO \rightarrow β -LUMO (31.61%) β -HOMO \rightarrow β -LUMO+1 (6.64%)	
	TD-M062X/6-31G*	EtOH	2.28	544	1.9461	α -HOMO \rightarrow α -LUMO (27.42%) α -SOMO \rightarrow α -LUMO (21.33%) β -HOMO \rightarrow β -LUMO +1 (46.41%)	1.63	762	0.3756	α -SOMO \rightarrow α -LUMO+2 (12.04%) β -HOMO \rightarrow β -SOMO (82.68%)
							2.58	480	1.9499	α -SOMO \rightarrow α -LUMO+2 (77.94%) β -HOMO \rightarrow β -SOMO (12.04%)
None		2.29	542	1.8462	α -HOMO-1 \rightarrow α -LUMO+1 (1.30%) α -HOMO \rightarrow α -LUMO (49.94%) β -HOMO-1 \rightarrow β -LUMO+1 (1.1%) β -HOMO \rightarrow β -SOMO (46.22%)	1.62	767	0.3108	α -SOMO \rightarrow α -LUMO+3 (13.53%) β -HOMO \rightarrow β -SOMO (79.63%)	
						2.63	465	1.7330	α -SOMO \rightarrow α -LUMO+3 (69.97%) β -HOMO \rightarrow β -SOMO (12.56%)	
TD-PBE0/6-31G*	EtOH	2.16	574	2.0300	α -HOMO \rightarrow α -LUMO (47.90%) α -SOMO \rightarrow α -LUMO (2.90%) β -HOMO \rightarrow β -SOMO (49.01%)	1.71	726	0.2203	α -SOMO \rightarrow α -LUMO+2 (20.41%) β -HOMO \rightarrow β -SOMO (76.39%)	
						2.42	512	2.0344	α -SOMO \rightarrow α -LUMO+2 (68.97%) β -HOMO \rightarrow β -SOMO (20.33%)	
	None	2.25	551	1.8667	α -HOMO \rightarrow α -LUMO (50.20%) β -HOMO \rightarrow β -SOMO (49.51%) β -HOMO \leftarrow β -SOMO (1.06%)	1.53	811	0.1454	α -SOMO \rightarrow α -LUMO (11.09%) α -SOMO \rightarrow α -LUMO+3 (10.37%) β -HOMO \rightarrow β -LUMO (71.50%)	

						2.44	508	0.9514	α -SOMO \rightarrow α -LUMO+3 (36.78%) β -HOMO \rightarrow β -LUMO (25.91%) β -HOMO \rightarrow β -LUMO+1 (19.58%)
TD-WB97XD/6-31G*	EtOH	2.27	546	2.0903	α -SOMO \rightarrow α -LUMO (46.03%) β -HOMO \rightarrow β -SOMO (45.74%)	1.90	651	0.3232	α -SOMO \rightarrow α -LUMO+2 (12.53%) β -HOMO \rightarrow β -SOMO (76.02%)
						2.69	460	1.9252	α -SOMO \rightarrow α -LUMO+2 (69.77%) β -HOMO \rightarrow β -SOMO (13.68%)
	None	2.32	533	1.9332	α -HOMO-1 \rightarrow α -LUMO+1 (1.87%) α -HOMO \rightarrow α -LUMO (2.98%) α -SOMO \rightarrow α -LUMO (44.98%) β -HOMO-1 \rightarrow β -LUMO+1 (1.73%) β -HOMO \rightarrow β -SOMO (46.13%)	1.87	662	0.2899	α -SOMO \rightarrow α -LUMO+3 (13.03%) β -HOMO \rightarrow β -SOMO (38.69%) β -HOMO \rightarrow β -LUMO (37.87%)
						2.71	452	1.6290	α -SOMO \rightarrow α -LUMO+3 (55.77%) β -HOMO \rightarrow β -LUMO (12.24%)

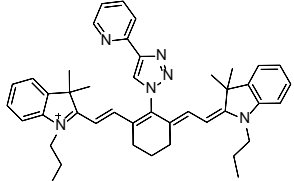
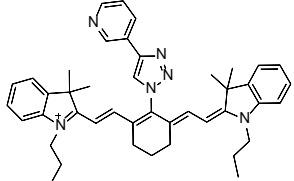
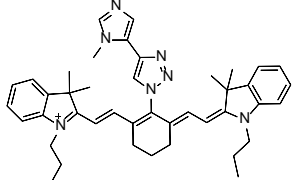
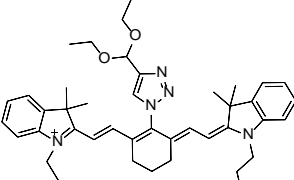
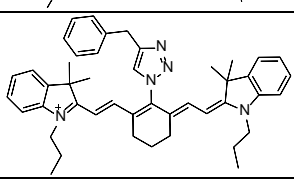
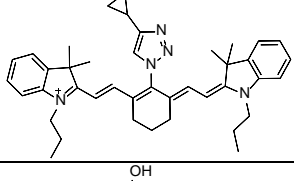
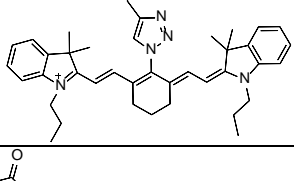
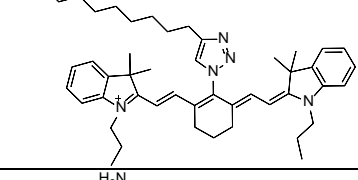
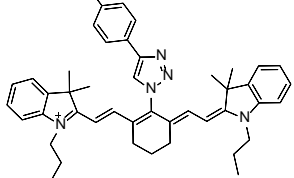
Table S2. Chemical and spectral characterisation data for the CIR fluorophores.

Compound code	Chemical structure	M _{calc.} [M+H] ⁺ _{exp.}	tR ⁺ (purity)	Yield (%)	λ _{exc.} (nm)	λ _{em.} (nm)	QY*
2		648.4 (648.5)	7.75 (100%)	48	803	840	10
CIR1		678.4 (678.3)	7.06 (100%)	55	802	839	10
CIR2		614.4 (614.6)	7.88 (98%)	37	801	831	14
CIR3		714.5 (714.5)	7.90 (97%)	17	801	835	18
CIR4		656.5 (656.5)	8.16 (98%)	18	800	839	11
CIR6		662.4 (662.4)	7.98 (100%)	34	802	833	13
CIR7		698.4 (698.4)	8.08 (100%)	19	802	840	14
CIR8		676.4 (676.4)	7.77 (100%)	16	801	839	15
CIR9		748.4 (748.3)	8.61 (100%)	18	803	835	12

CIR10		664.4 (664.5)	7.17 (100%)	13	802	834	13
CIR11		663.4 (663.5)	7.59 (100%)	11	803	840	6
CIR12		676.4 (676.5)	7.59 (100%)	18	804	840	9
CIR13		678.4 (678.4)	7.57 (100%)	14	802	838	11
CIR14		679.8 (680.4)	7.55 (42%)	19	802	839	9
CIR15		691.4 (691.5)	7.68 (100%)	14	802	839	6
CIR16		716.4 (716.3)	7.98 (100%)	12	803	838	10
CIR17		726.3 (726.3)	7.98 (100%)	20	802	840	13
CIR18		692.4 (692.4)	7.13 (100%)	12	803	836	13

CIR19		666.4 (666.5)	7.76 (100%)	48	802	832	12
CIR20		716.4 (716.5)	7.89 (85%)	27	807	840	10
CIR21		693.4 (693.4)	7.61 (100%)	19	803	839	9
CIR22		714.4 (714.4)	7.63 (100%)	42	803	839	10
CIR23		731.4 (731.5)	7.61 (100%)	13	802	836	1
CIR24		704.4 (704.4)	8.48 (100%)	16	802	840	9
CIR25		616.4 (616.4)	6.81 (100%)	30	800	829	14
CIR26		682.4 (682.4)	7.77 (100%)	16	803	840	9
CIR27		640.4 (640.5)	7.77 (100%)	14	800	840	14

CIR28		654.4 (654.4)	8.10 (89%)	33	800	833	14
CIR29		684.4 (684.4)	7.93 (100%)	25	803	838	13
CIR30		754.4 (754.5)	7.93 (100%)	33	803	835	13
CIR31		678.4 (678.5)	7.80 (95%)	31	803	838	11
CIR32		784.4 (784.3)	8.33 (100%)	21	804	840	11
CIR33		740.4 (740.3)	8.11 (100%)	28	803	840	13
CIR34		672.4 (672.5)	6.95 (100%)	13	801	833	15
CIR35		644.4 (644.3)	6.80 (100%)	26	801	838	15
CIR36		630.4 (630.3)	6.95 (100%)	52	801	831	19
CIR37		654.4 (654.3)	7.54 (94%)	38	803	832	14

CIR38		649.4 (649.5)	7.41 (100%)	22	804	840	15
CIR39		649.4 (649.4)	7.13 (100%)	32	803	835	13
CIR40		652.4 (652.5)	6.37 (69%)	14	803	835	13
CIR41		674.4 (674.5)	7.55 (100%)	36	803	838	13
CIR42		662.4 (662.4)	7.59 (100%)	33	802	838	13
CIR43		612.4 (612.4)	7.31 (100%)	35	801	835	15
CIR44		602.4 (602.4)	6.81 (100%)	55	801	835	14
CIR45		728.4 (728.6)	7.41 (100%)	3	801	832	18
CIR46		663.4 (663.5)	7.09 (100%)	2	802	835	4

* Retention time and UV-based purity were determined under the HPLC conditions described in the Experimental Section. * Wavelengths and fluorescence quantum yields determined in DMSO using ICG (in DMSO, QY: 12%) as the reference standard.

Table S3. HRMS characterisation of the CIR library.

Compound code	M_{calc.}	M_{exp.}
2	648.4061	648.4069
CIR1	678.4166	678.4196
CIR2	614.4217	614.4237
CIR3	714.5106	714.5107
CIR4	656.4687	656.4692
CIR6	662.4217	662.4254
CIR7	698.4217	698.4218
CIR8	676.4373	676.4379
CIR9	748.4373	748.4368
CIR10	664.4010	664.4015
CIR11	663.4169	663.4168
CIR12	676.4009	676.4002
CIR13	678.4166	678.4223
CIR14	678.3166	678.3184
CIR15	691.4482	691.4487
CIR16	716.3935	716.3939
CIR17	726.3166	n.d.
CIR18	692.3959	692.3974
CIR19	666.3966	666.3953
CIR20	716.3935	716.3938
CIR21	693.3912	693.3913
CIR22	714.3978	714.3976
CIR23	731.4796	731.4828
CIR24	704.4687	704.4664
CIR25	616.4010	616.4033
CIR26	682.3671	682.3687
CIR27	640.4374	640.4374
CIR28	654.4530	654.4582
CIR29	684.3872	684.3868
CIR30	754.4479	754.4449
CIR31	678.4166	678.4175
CIR32	784.3808	784.3834
CIR33	740.4323	740.4322
CIR34	672.4272	672.4275
CIR35	644.3959	644.3962
CIR36	630.4166	630.4184
CIR37	654.3625	654.3637
CIR38	649.4013	649.4029
CIR39	649.4013	649.4020
CIR40	652.4122	652.4152
CIR41	674.4428	674.4427
CIR42	662.4217	662.4246
CIR43	612.4061	612.4122
CIR44	602.3853	602.3843
CIR45	728.3898	728.3347
CIR46	663.4170	663.4168

Table S4. Spectral properties of heptamethine and cyanine dyes.

Compound	$\lambda_{\text{exc.}}$ (nm)	$\lambda_{\text{em.}}$ (nm)	QY (%)	ϵ ($\text{M}^{-1} \text{cm}^{-1}$)	Photostability (%)
CIR38(M)	796	818	19 \pm 4	238,000	91 \pm 9
IR780	785	806	9 \pm 2	345,000	64 \pm 2
IR800CW-SE	785	806	16 \pm 1	295,000	93 \pm 2
IR783	786	810	15 \pm 2	224,000	95 \pm 2

Fluorescence quantum yields determined in DMSO using ICG (in DMSO, QY: 12%) as the reference standard. Wavelengths and extinction coefficients determined in EtOH. Photostability indicated as means \pm s.e.m of chemical integrity after 12 h irradiation (50 μM PBS) (n=5).

Table S5. Biochemical analysis of serum from mice injected with unlabelled or **CIR38M**-labelled CD4+ T cells. All values are represented as means \pm s.e.m and no significant statistical differences were observed between both groups ($p > 0.05$).

Biomarker	PBS	CIR38M
Cholesterol (mmol L ⁻¹)	2.22 \pm 0.21	2.51 \pm 0.09
Amylase (U L ⁻¹)	1580 \pm 99	2410 \pm 538
Alanine transaminase (U L ⁻¹)	56 \pm 24	54 \pm 19
Aspartate transaminase (U L ⁻¹)	135 \pm 42	167 \pm 30
Alkaline phosphatase (U L ⁻¹)	81 \pm 12	61 \pm 3
Albumin (g L ⁻¹)	22.80 \pm 0.75	22.50 \pm 0.63
Urea (mmol L ⁻¹)	7.90 \pm 0.21	8.97 \pm 0.32
Creatinine (μ mol L ⁻¹)	<10	<10
Triglyceride (mmol L ⁻¹)	1.88 \pm 0.00	2.08 \pm 0.23
Calcium (mmol L ⁻¹)	2.75 \pm 0.08	2.82 \pm 0.03
Phosphate (mmol L ⁻¹)	3.91 \pm 0.36	3.87 \pm 0.08
Creatine kinase (U L ⁻¹)	411 \pm 193	451 \pm 80
Total bilirubin (mmol L ⁻¹)	2.90 \pm 0.92	4.37 \pm 0.57